THE DESIGN AND CONSTRUCTION OF AN ON - LINE CONVERSION ELECTRON SPECTROMETER

Thesis for the Degree of M. S.

MICHIGAN STATE UNIVERSITY
LAWRENCE L. KNEISEL

1975

ABSTRACT

THE DESIGN AND CONSTRUCTION OF
AN ON-LINE CONVERSION ELECTRON SPECTROMETER

By

Lawrence L. Kneisel

An on-line conversion electron spectrometer was designed and built to supplement γ-ray research at the Michigan State University Cyclotron Laboratory. A short solenoidal magnet with anti-positron vanes was built into the system to enhance counting rates and to provide gross momentum selection. The system was initially tested with a low resolution surface barrier detector. Later a high resolution, Si(Li) detector was used to obtain electron spectra for ^{154}Gd and $^{117,\ 118}$Sb using the reactions ^{154}Sm $(\alpha, 4n\gamma)^{154}$Gd and $^{117,\ 118}$Sn $(p, n\gamma)^{117,\ 118}$Sb.

THE DESIGN AND CONSTRUCTION OF AN ON-LINE CONVERSION ELECTRON SPECTROMETER

By

Lawrence L. Kneisel

A THESIS

Submitted to

Michigan State University

in partial fulfillment of the requirements

for the degree of

MASTER OF SCIENCE

Department of Physics

1975

To Jan

ACKNOWLEDGMENTS

I wish to acknowledge my advisor, Dr. W.H. Kelly, for his patience and help in writing this thesis.

I wish to particularly thank Dr. R.A. Warner for all his time that he unselfishly spent with me during the design and testing period of this project. His suggestions and guidance played a large part in its successful completion. I do not know how he could survive those all night experiments and still appear completely normal the next day. I want to thank Drs. F.M. Bernthal and Khoo T.L. for their help in choosing the Si(Li) detector. I also want to thank Harold Hilbert and Mike Edmiston for their suggestions in design and construction.

This work was supported by grants from the National Science Foundation.

TABLE OF CONTENTS

LIST OF TABLES

LIST OF FIGURES

INTRODUCTION

1. Work Done at Michigan State University

Experimental gamma-ray spectroscopy at Michigan State University, performed under the direction of Profs. W.H. Kelly, Wm. McHarris and F.M. Bernthal has centered around the Michigan State University 163 cm sector focused cyclotron with supplemental experiments performed using the tandem Van de Graaff accelerator on the campus of Western Michigan University.

A γ-ray detector-electronic system has been developed to take advantage of the variety of beams produced by the cyclotron. Experiments are performed regularly using the techniques of γ-γ coincidences, angular distribution measurements, He-JRT thermalizer for radioactive decay, beam sweeping for lifetime measurements, and (p, xnγ) and (alpha-xnγ) reactions.

An on-line electron spectrometer has been built using a surface barrier detector to study internal conversion electrons. A short solenoidal magnet was constructed to enhance counting rates, to provide gross momentum selection and to remove unwanted signals from x-rays and low energy gamma-rays. To extend the range of the system, the magnetic field is swept using a wave from a wave generator. A single channel analyzer and a computer program are used to create a narrow band width detection system that is swept with the field. The system was tested with a ^{154}Sm (α, 4nγ)^{154}Gd and $^{116, 117, 118}$Sn (p, nγ) $^{116, 117, 118}$Sb

experiments. The design, construction and testing of this conversion electron spectrometer is the subject of this thesis.

2. Cyclotron Description and Transport System

The 48 MeV alpha and 10 MeV proton beams used in the testing of the spectrometer were produced by the Michigan State University cyclotron. This is a variable energy cyclotron capable of producing 25-48 MeV alphas of high resolution. Other particles that can be produced include p, d, ^{3}He, and ^{12}C. (Bl 66) The beams are extracted in a two stage process; a field bump in conjunction with a conventional electrostatic deflector, followed by a magnetic channel that focuses the beam, with the help of a bending magnet (MV1), during the final transversal of the fringe field.

Upon extraction, a series of bending magnets (M1, M2, MV1), and quadrupoles (Q_1, Q_2), align the beam parallel with the beam pipe axis and center it at Box 4 (Figure 1) where an adjustment of the beam intensity can be made by movable slits. The 45° bending magnets (M3, M4), along with the quadrupoles (Q_5, Q_6), form an analysis system for the beam, while a sextupole removes some systemic aberration in the analysis magnets. Boxes 5 and 6 form the object and image slits for the system. At M5 the beam is switched to the +45° beam-line where it is focused on the target by quadrupoles (Q_9, Q_{10}).

3. Experimental Area

The γ-γ coincidence chamber was modified to accept the electron spectrometer. This chamber is mounted on the goniometer arm and attached to the beam pipe (Figure 2).

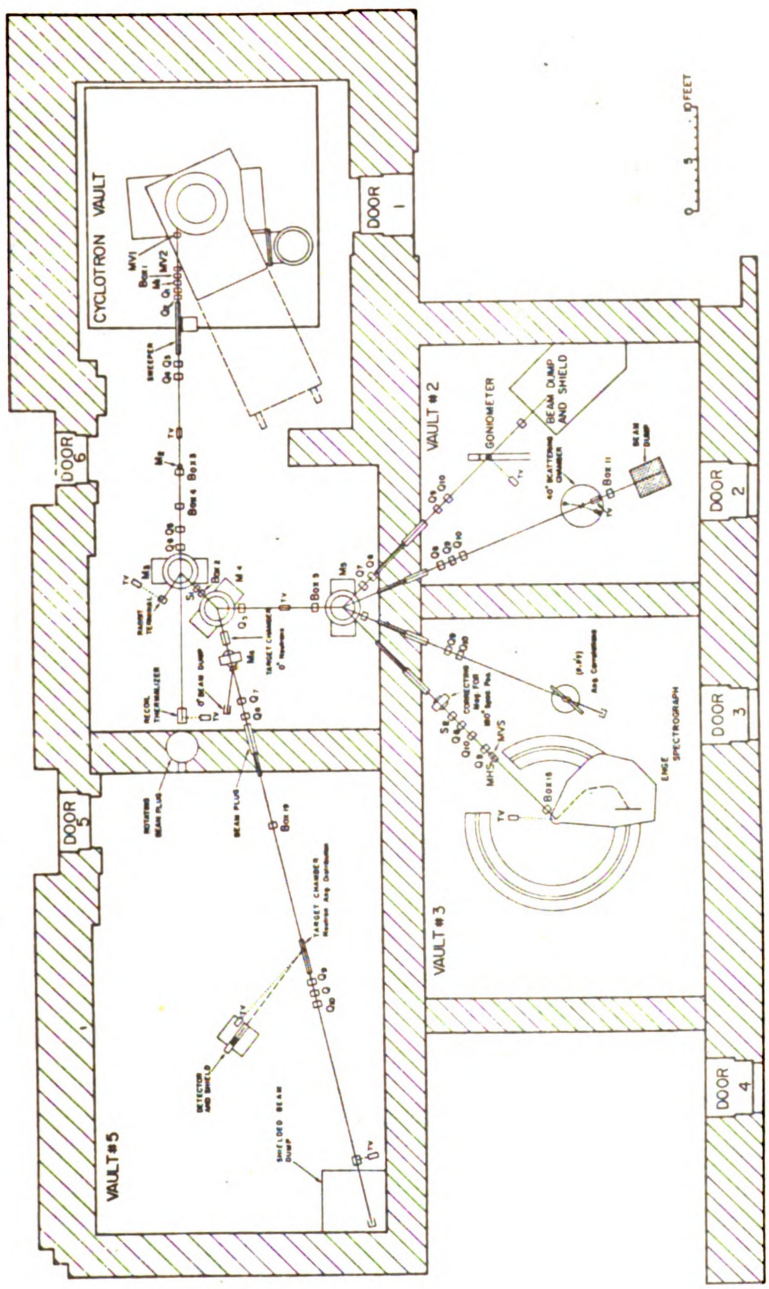

Figure 1. Cyclotron And Beam Transport

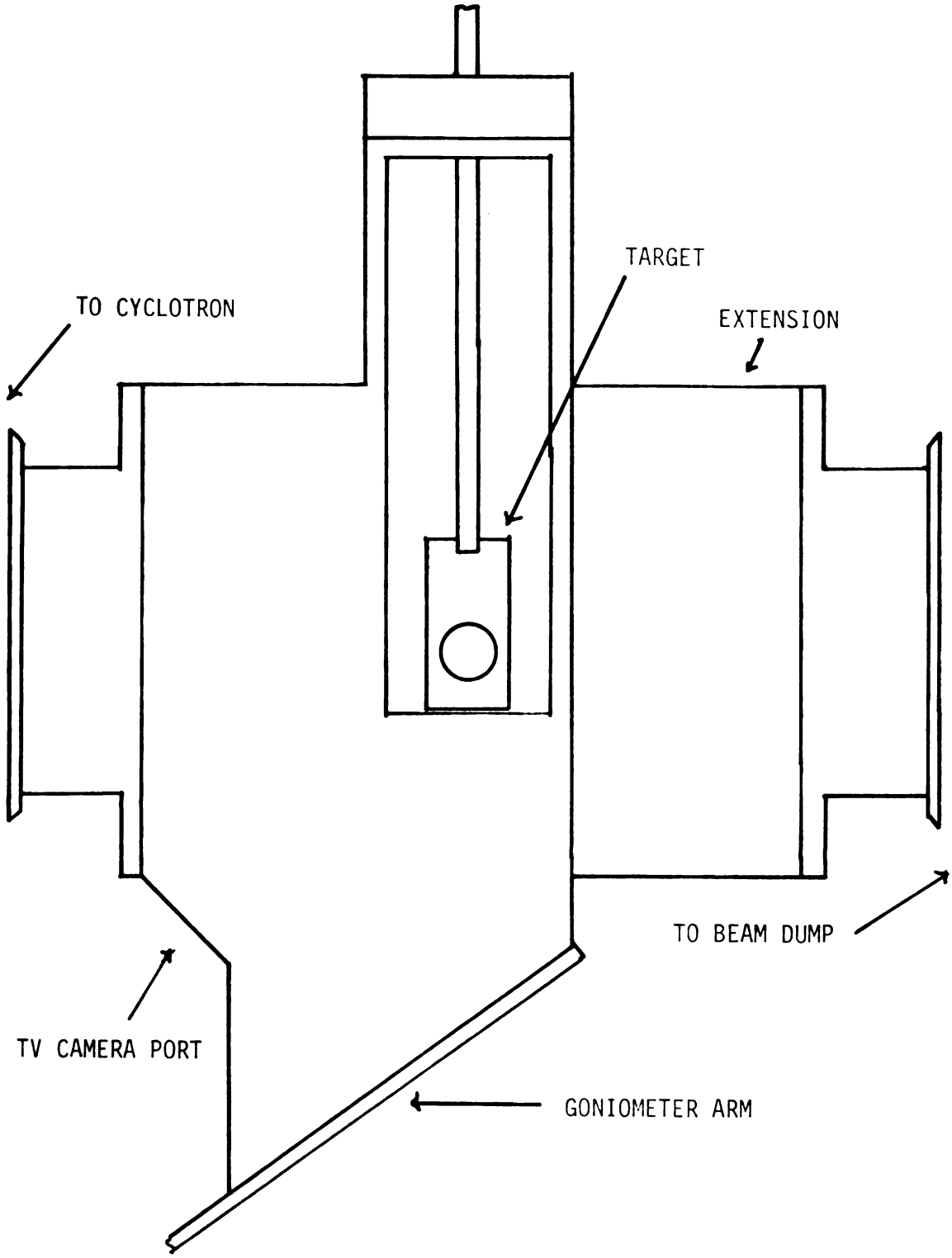

Figure 2. γ-γ Coincidence Chamber with Modifications

The coincidence chamber is constructed of ultra-pure aluminum and protected from the beam with lead at the entrance and exit ports. A television camera is mounted below to provide for visual alignment and focusing of the beam. The opposing window design allows electron and gamma spectra to be taken simultaneously. The target area is at beam-line vacuum (~1μ), provided by a 3" diffusion pump upstream from the chamber (Figure 3). The exit port was lengthened to provide clearance from the solenoid and one window was replaced by a mating plate for the spectrometer

4. Internal Conversion Processes

When a nucleus is in an excited state at energies insufficient for nuclear particle emission, two processes compete, photon emission and electron conversion. A branching ratio, α, can be defined for a transition as the ratio of the number of conversion electrons, N_e, divided by the number of photons, N_γ, emitted in the same time interval.

$$\alpha = \frac{N_e}{N_\gamma}$$

α then corresponds to a probability ratio of the two processes. It can be shown that:

$$\lambda = \lambda_\gamma(1 + \alpha)$$

where λ is the decay constant for the excited state and γ is the constant for γ-ray decay.

The energy of the conversion electron can be expressed as:

$$K.E. = W_i - W_f - E.B.$$

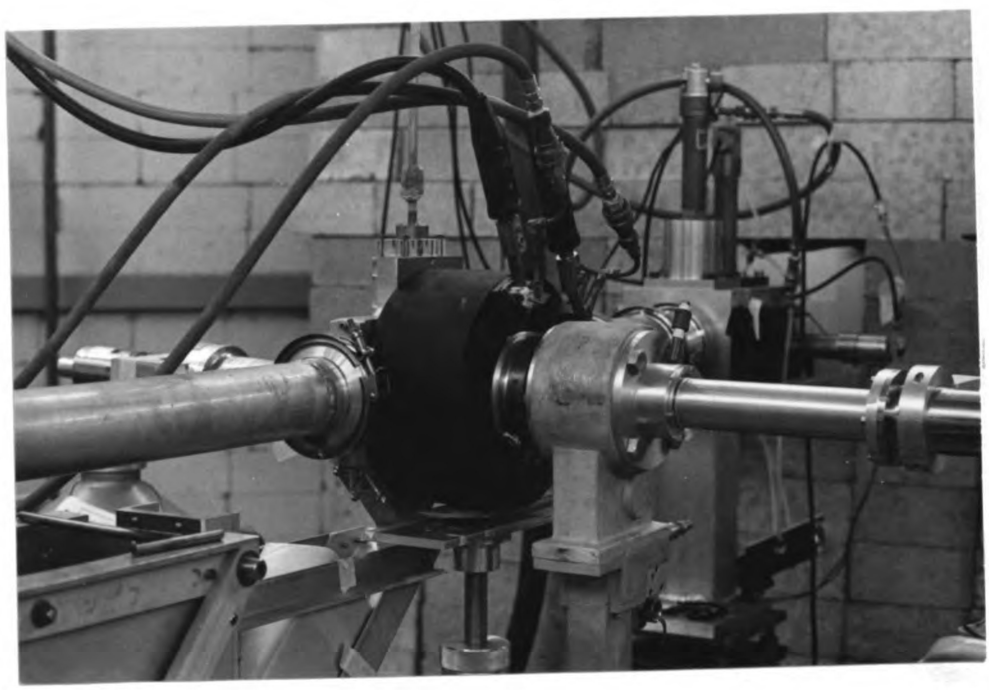

Figure 3. Spectrometer In Place on Beam Line

where E.B. is the binding energy of the atomic electron and W_i and W_f are the initial and final energy levels respectively. If a detector has sufficient resolution, the resulting spectrum will have an individual peak for each shell (K, L_I, L_{II}, L_{III}, etc.), for each transition. For example, consider ^{214}Po, the binding energies are E_k = 93.1 keV; E_{L_I} = 16.9 keV; E_{M_I} = 4.2 keV; a detector with 10 keV resolution could be used to determine K/L ratios with a minimal amount of trouble. (Le 67)

The theory of internal conversion shows an expression for the decay constant, λ_e, that contains the same matrix elements as the expressions for λ_γ. This means that the conversion coefficients, α_K, α_L, α_M, depend exclusively upon the type of transition (E or M), the multipolarity, the nuclear charge and the transition energy.

Blatt and Weisskopf (Bl 52) show an approximate formula for the K electron conversion of multipolarity ℓ:

$$\alpha_K = z^3 \left[\frac{e^2}{4\pi\varepsilon_o hc}\right]^4 \frac{\ell}{\ell+1} \left[\frac{2m_o c^2}{h\omega}\right]^{\ell + 5/2}$$

The factor raised to the fourth power is the fine structure constant. This approximation is not applicable for low energy transitions in heavy nuclei. More elaborate calculations have been performed by Rose (Ro 68) and Hager and Selzer (Ha 68). Their publications include tables of coefficients for determination of multipolarities from experimental data. If one examines these tables, it can be seen that experimental measurements can be accurate enough to allow the determination of the multipolarity of the transition. It is sometimes simpler and more accurate to measure the K/L ratio.

where E.B. is the binding energy of the atomic electron and W_i and W_f are the initial and final energy levels respectively. If a detector has sufficient resolution, the resulting spectrum will have an individual peak for each shell (K, L_I, L_{II}, L_{III}, etc.), for each transition. For example, consider ^{214}Po, the binding energies are E_k = 93.1 keV; E_{L_I} = 16.9 keV; E_{M_I} = 4.2 keV; a detector with 10 keV resolution could be used to determine K/L ratios with a minimal amount of trouble. (Le 67)

The theory of internal conversion shows an expression for the decay constant, λ_e, that contains the same matrix elements as the expressions for λ_γ. This means that the conversion coefficients, α_K, α_L, α_M, depend exclusively upon the type of transition (E or M), the multipolarity, the nuclear charge and the transition energy.

Blatt and Weisskopf (Bl 52) show an approximate formula for the K electron conversion of multipolarity ℓ:

$$\alpha_K = z^3 \left[\frac{e^2}{4\pi\varepsilon_o hc}\right]^4 \frac{\ell}{\ell+1} \left[\frac{2m_o c^2}{h\omega}\right]^{\ell + 5/2}$$

The factor raised to the fourth power is the fine structure constant. This approximation is not applicable for low energy transitions in heavy nuclei. More elaborate calculations have been performed by Rose (Ro 68) and Hager and Selzer (Ha 68). Their publications include tables of coefficients for determination of multipolarities from experimental data. If one examines these tables, it can be seen that experimental measurements can be accurate enough to allow the determination of the multipolarity of the transition. It is sometimes simpler and more accurate to measure the K/L ratio.

DESIGN AND CONSTRUCTION

1. Electron Trajectory Theory

To compensate for low counting rates from the thin targets, a short solenoidal magnet was built. An idealized magnet and electron trajectory are shown in Figures 4 and 5. The treatment follows that of J.E. Draper of the University of California at Davis. (Wy 71) The idealized magnet is defined as having the magnetic field of an infinite solenoid with no fringing fields, i.e., the field is uniform in the region labeled B in Figure 4 and nonexistent everywhere else. An electron moving through a magnetic field has a cyclotron frequency of ω. The angle through which the electron rotates is

$$\Phi = \omega t \tag{1}$$

where t is the time the electron spends in the field. From Figure 4, it can be seen that the electron trajectory when viewed down the axis of the coil is

$$\Phi = \omega t = \left[\frac{Be}{M}\right]\left[\frac{L}{V_H}\right] \tag{2}$$

where m is electron mass, L is the length of the solenoid, V_H is electron velocity parallel to the field, B is magnetic field strength and e is electron charge. A function, f, can be defined such that

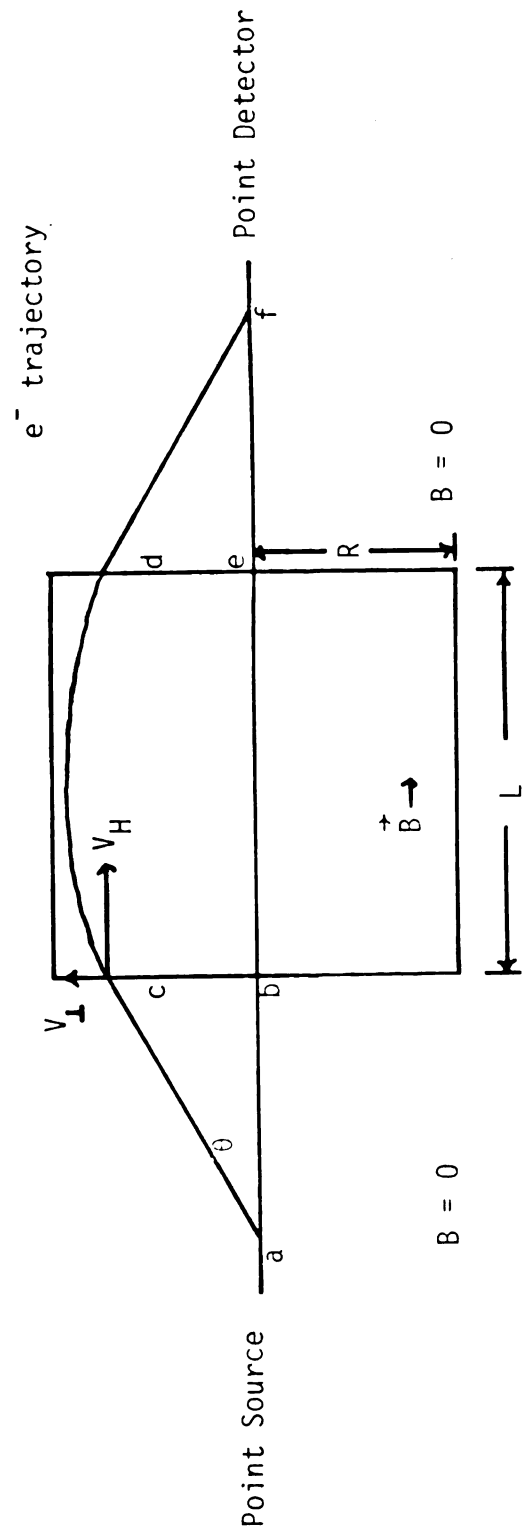

Figure 4. Idealized Magnet and Electron Trajectory

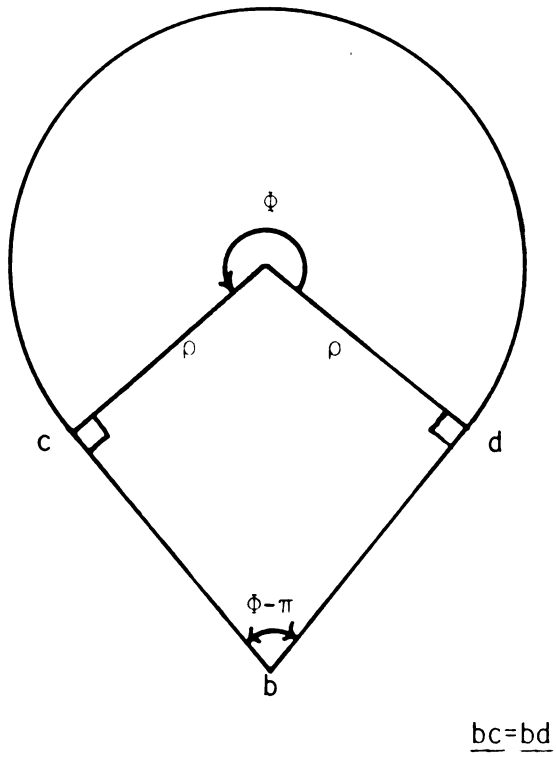

Figure 5. View of Electron Trajectory Looking Down Spectrometer Axis (Axis is Point b)

$$\Phi \equiv \pi f \tag{3}$$

and geometrically from Figure 5

$$\Phi = \pi + 2\tan^{-1}\left[\frac{\rho}{\underline{bc}}\right] \tag{4}$$

where $\underline{bc}$ is the distance the electron drifts with no field acting upon it and ρ is the radius of curvature in the field. Using Equation 3 gives

$$f = 1 + \frac{2}{\pi}\tan^{-1}\left[\frac{\rho}{\underline{bc}}\right]. \tag{5}$$

Rearranging Equation 2 and using the substition of Equation 3 gives

$$V_H = \frac{BeL}{m\pi f} \tag{6}$$

which can also be written as

$$V_H = V\cos\theta. \tag{7}$$

Since the momentum is $p = mV$, rearrangement of Equations 6 and 7 gives

$$p = mV = \frac{BeL}{\pi f\cos\theta}. \tag{8}$$

It is known that the radius of curvature in a magnetic field, ρ, is related to the perpendicular component of the momentum,

$$p = mV = eB\rho. \tag{9}$$

Rearrangement of terms gives

$$\rho = \frac{p}{eB}\left[\frac{p \sin \theta}{eB}\right], \tag{10}$$

so

$$\frac{\rho}{\underline{bc}} = \frac{p \sin \theta}{eB \tan \theta} \quad . \tag{11}$$

But from Equation 8, the momentum that the electron requires to reach the detector replaces p in Equation 11 and gives

$$\frac{\rho}{\underline{bc}} = \left[\frac{BeL}{\pi f \cos \theta}\right] \left[\frac{\sin \theta}{eB\underline{ab} \tan \theta}\right] \tag{12}$$

or

$$\frac{\rho}{\underline{bc}} = \frac{L}{\underline{ab}\ \pi f} \quad . \tag{13}$$

Substituting this into Equation 5 gives the transcendental equation

$$f = 1 + \frac{2}{\pi} \tan^{-1}\left[\frac{L}{\underline{ab}\ \pi f}\right] \quad . \tag{14}$$

This transcendental equation shows that f depends on geometry i.e., L/ab. A graphical solution is shown in Figure 6. From the solution of f, Φ is easily found and the field required for a specific energy and take-off angle, θ, can be solved. The fact that the trajectory must miss the coil requires an upper limit, θ_{max}. This is the take-off angle for which the electron just grazes the inner wall of the vacuum chamber.

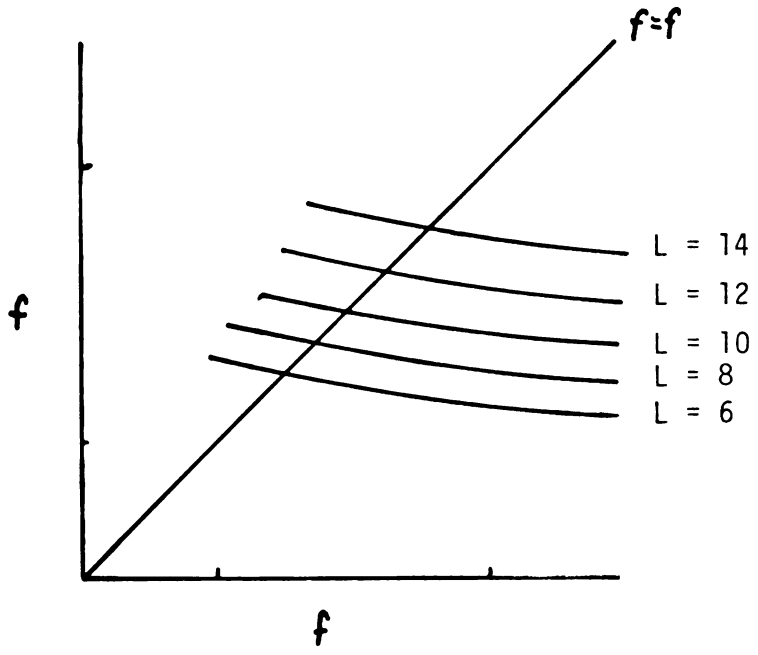

Figure 6. Graphical Solution of Transcendental Equation

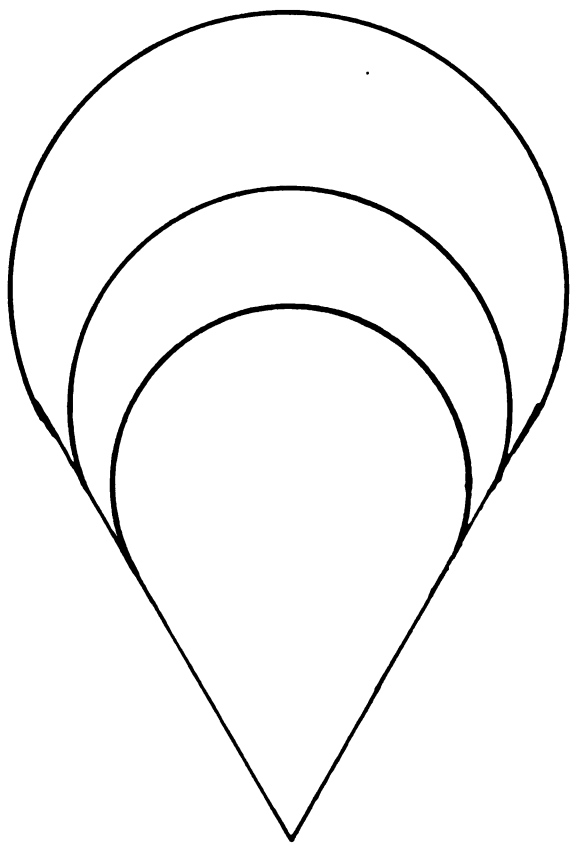

Figure 7. Electron Trajectories Looking Down Spectrometer Axis For Different Energies and Magnet Settings

2. Construction of the Magnet

Usually arrangements are such that the target makes an angle of 45° to the beam axis and to the spectrometer axis. This angle was taken to be θ_{max} for this would correspond to the case of the electron just skimming the target surface. The length of the coil and maximum current were varied to determine the optimum size of the magnet with regard to the material weight, physical size, and the field needed to produce a target to detector trajectory for 2 MeV electrons. It was found that the length of the coil should be 10 cm with a maximum current of 150 amperes and 180 turns.

The solenoid was constructed from a single length of 2.7 mm square copper conductor with a 2 mm diameter hole for cooling water. This conductor was supplied with an epoxy and fabric insulation which prevented shorting between adjacent turns. The copper was wrapped around an aluminum cylinder which was doubly insulated from the coil with fiberglass tape. The completed coil was potted in epoxy resin and cured for 12 hours at 135° C. The outer parts of the assembly were made of cold rolled steel to shield the flight path from stray magnetic fields and to provide a flux return path which reduced bending of the cyclotron beam (Figure 8). A Marman flange attachment was mounted on the detector side of the magnet; the target side was polished for an O-ring seal.

3. Cooling Water

The water used for cooling was provided by the low conductivity water system already installed in the building. This system provided a 6.89×10^6 d/cm^2 pressure differential of deionized water across the magnet. The flow rate was calculated using the equation:

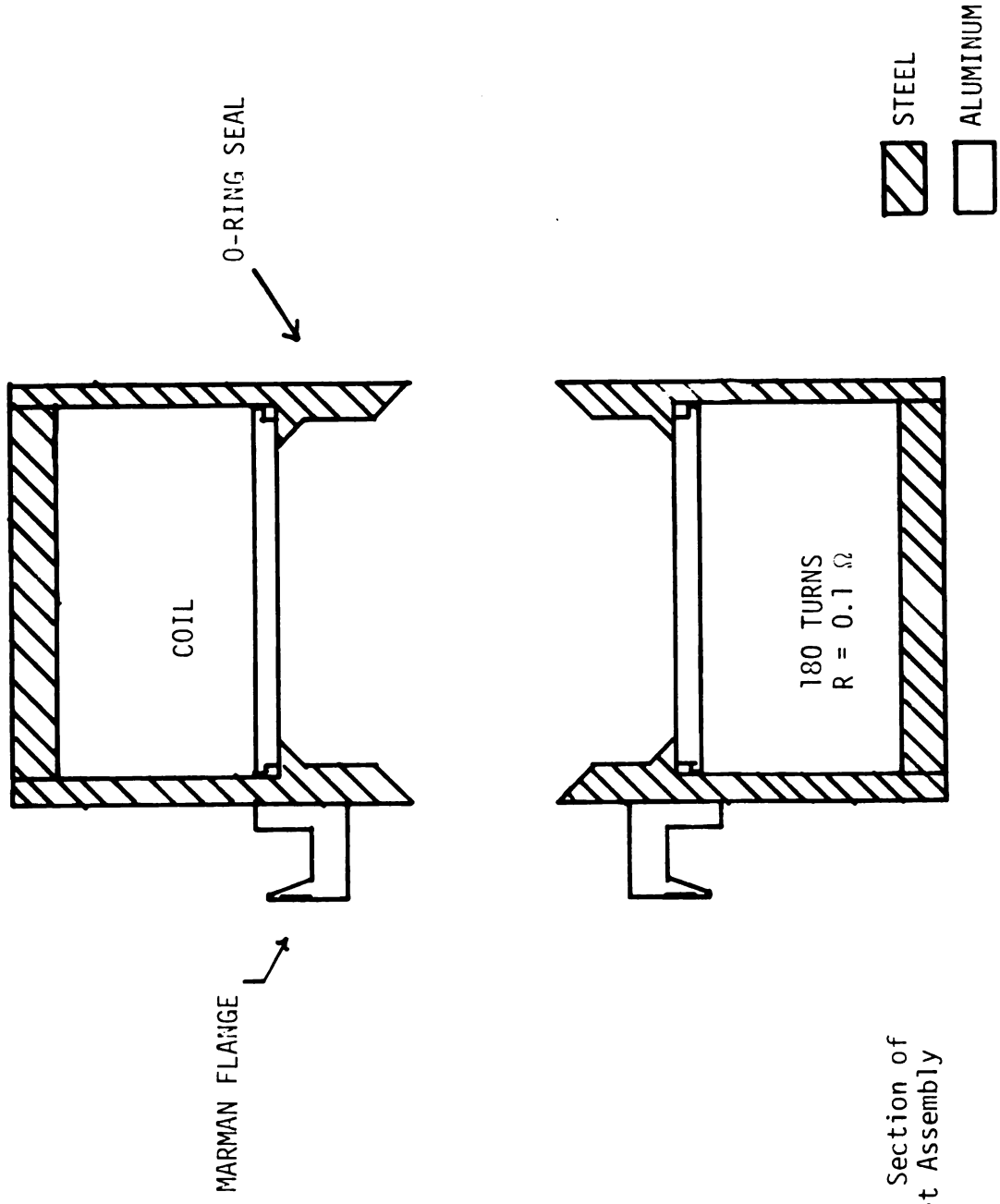

Figure 8. Cross Section of Magnet Assembly

$$v = \frac{Pr^4}{8Lm} \qquad \text{(Ch 72)}$$

where: v = velocity in cm^3/sec
P = Pressure in $dynes/cm^2$
L = Length of the conduit in cm
r = radius of the conduit in cm
m = viscosity of water in poise

The flow rate was converted to calories per minute per °C and divided into the I^2R losses of the coil. The results of these calculations for the temperature rise as a function of the magnet current are shown in Figure 9 for the average of the swept current. A temperature switch was mounted on the exit side of the cooling water. This switch opens at 60°C which corresponds to 75 amperes in Figure 9. This means that the maximum average current that can be tolerated is 75 amperes. With a sweep rate of 100 sec/cycle, the peak current must be under 125 amperes.

4. Power Supply

The current for the coil was provided by an unused quadrupole connection from a Perkin current supply. This supply is capable of providing a stable, regulated (1%) current of up to 200 amperes determined by a reference voltage of 0-9 volts at the control board. This reference voltage is supplied by an offset waveform from a Wavetec signal generator. Since the signal generator can provide a maximum signal of 3 volts, this signal is amplified and offset by an operational amplifier. The magnetic field was measured with a rotating coil gaussmeter 1 cm inside the coil for different current settings. The results are shown in Figure 10. For a 2 MeV electron with a take-off angle of 45°, a B field of 6.43 KGauss is needed to enable the electron to reach the detector.

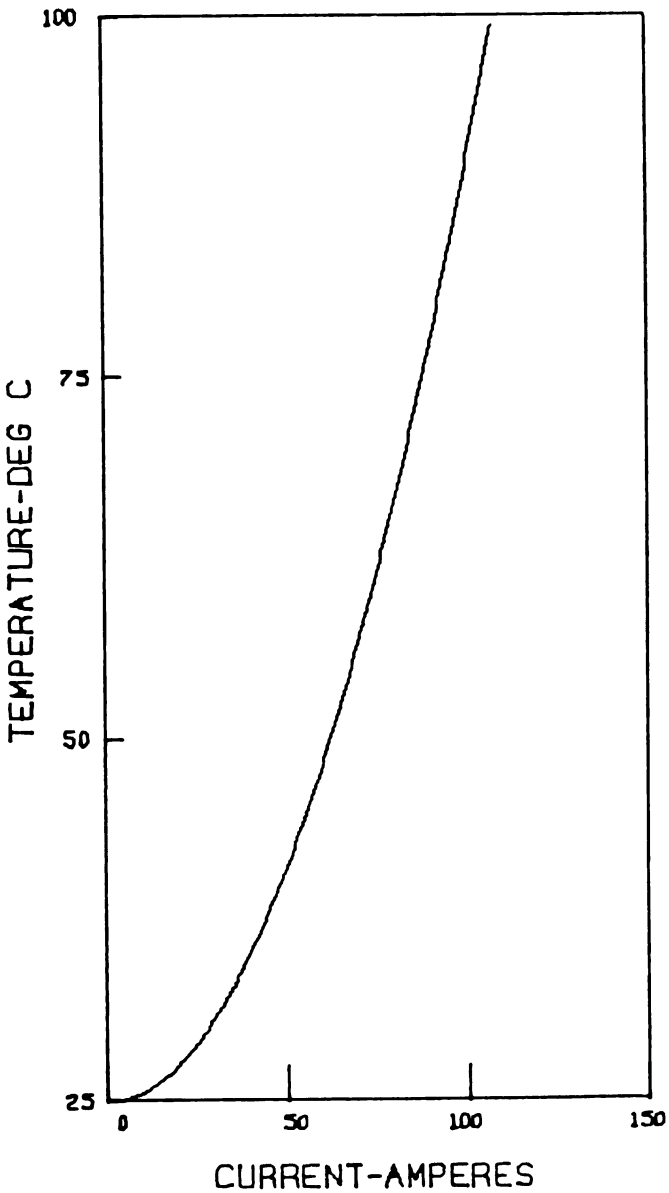

Figure 9. Water Temperature As A Function of Magnet Current (Water Is 25° C At Input)

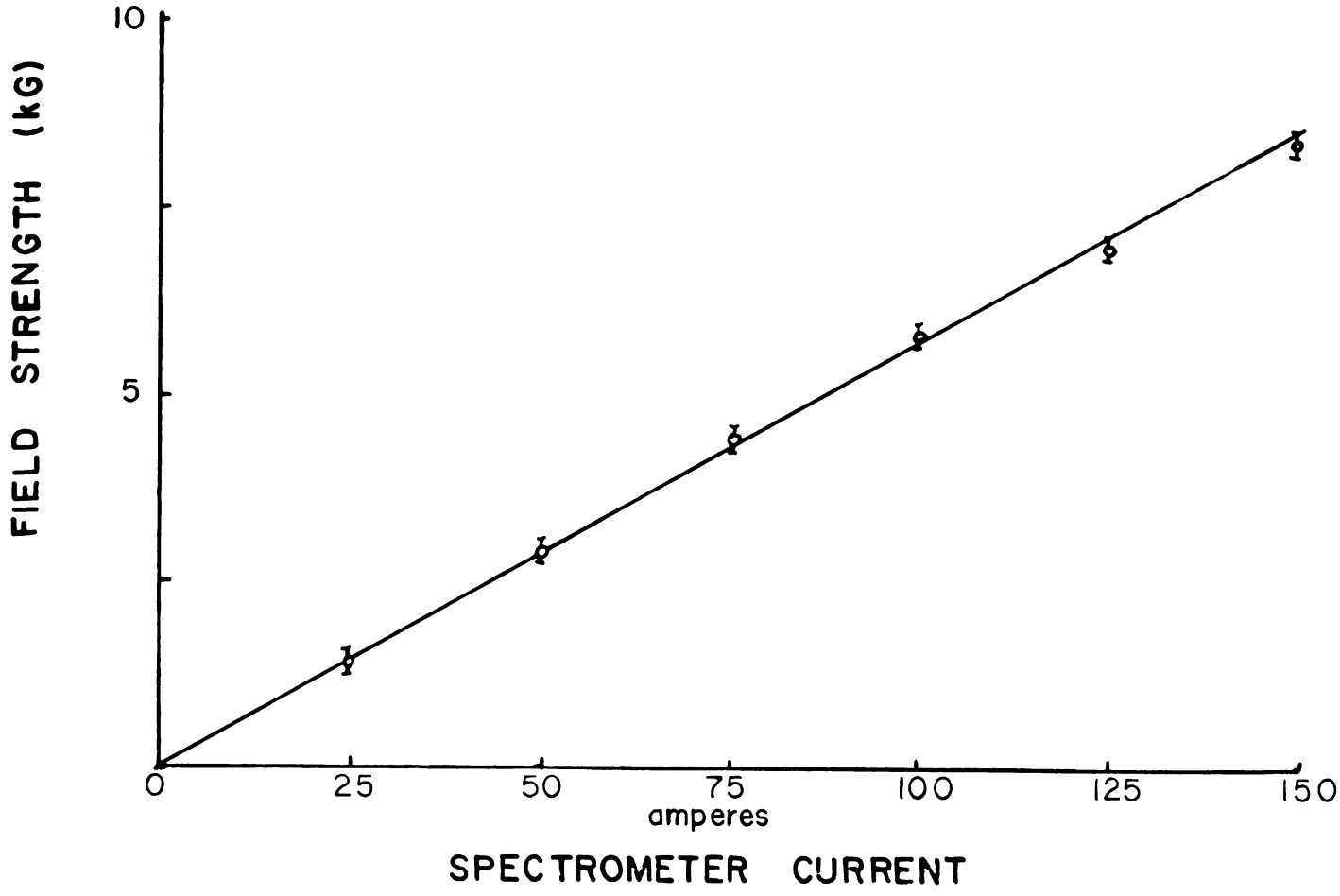

Figure 10. Field Strength as a Function of Spectrometer Current

It can be seen that a current of 110 amperes is needed for this to occur. Thus, this represents the approximate, maximum energy electrons that can be studied with the spectrometer.

5. Anti-positron Vanes

Anti-positron vanes were installed to prevent unwanted counts from positrons, which because of their opposite charge, from spiraling in the direction opposite to that of the electrons. Before the vanes could be constructed, a test was performed on the coil to confirm the calculated electron path that spiraled through the vacuum chamber.

As was shown in Equation 4 in Section 3, the shape of the electron trajectory (and therefore the angle θ), is independent of the electron's momentum and the field strength. Therefore, a thin current-carrying wire, anchored at the detector and source positions, would assume the shape of the trajectory. In this way the effects of any nonconformity of the field can be determined. A thin copper wire of diameter 50 μm was used and a current of ~1 ampere was passed through it. The result was a pitch of 48.3 cm which implied $\Phi = 1.45\pi$ radians. Pitch is defined as the distance required for a spiral to have rotated 360° upon its axis. This agrees well with the calculated result which was 1.45π radians.

Upon completion of this test confirming the electron path, the vanes were constructed. The vanes form a helix about the axis of the coil. In order to cut the vanes from sheet lead, this helix must be unwound and laid out on a flat surface. Figure 11 defines the parameters used in the design of the vanes.

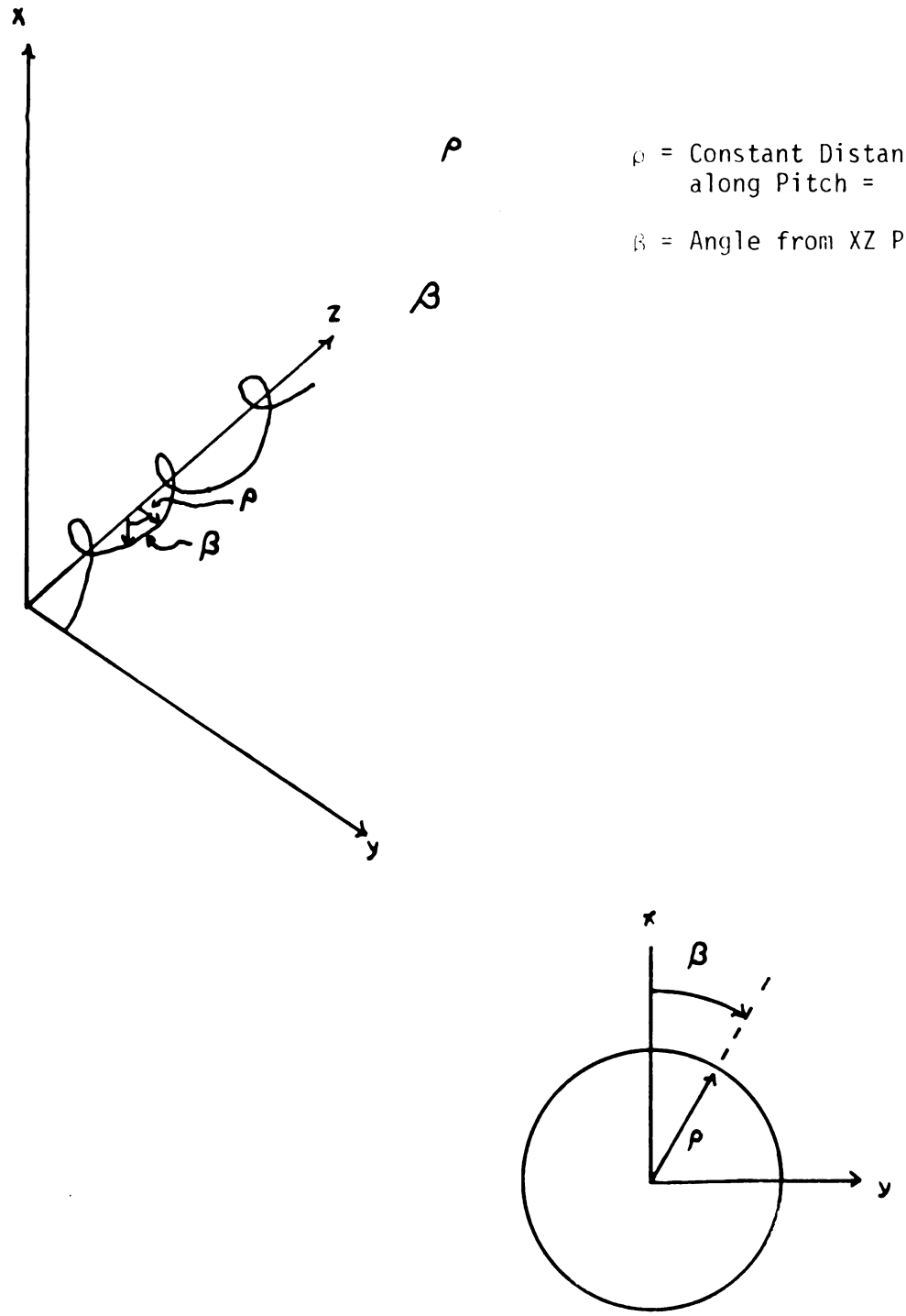

Figure 11. Geometrical Parameters Of a Helix

If dL is an element of path length along the helix then:

$$dL = \sqrt{dz^2 + (\rho d\beta)^2}$$

If P is the pitch of the helix then:

$$dz = \frac{P}{2\pi} \, d\beta$$

Or

$$dL = \frac{1}{2\pi} \sqrt{P^2 + (2\pi\rho)^2} \, d\beta$$

Integrating from 0 to $\Phi-\pi$ gives:

$$L = \frac{\Phi-\pi}{2\pi} \sqrt{P^2 + (2\pi\rho)^2}$$

If L_o = Path length at the edge of the vane, i.e., $\rho = R$

And L_i = Path length at the axis of the vane, i.e., $\rho = 0$

Then a truncated pie section can be defined such that:

$$L_o = \alpha(r + R)$$

And

$$L_i = \alpha r$$

As shown in Figure 12. This is the unwound helix and was used as a template for the vanes. Four vanes were cut and bent from 1/16 inch lead sheet and soldered together. A plug was filleted along the axis having the diameter of the detector (1 cm). The assembled vanes are shown in Figure 13.

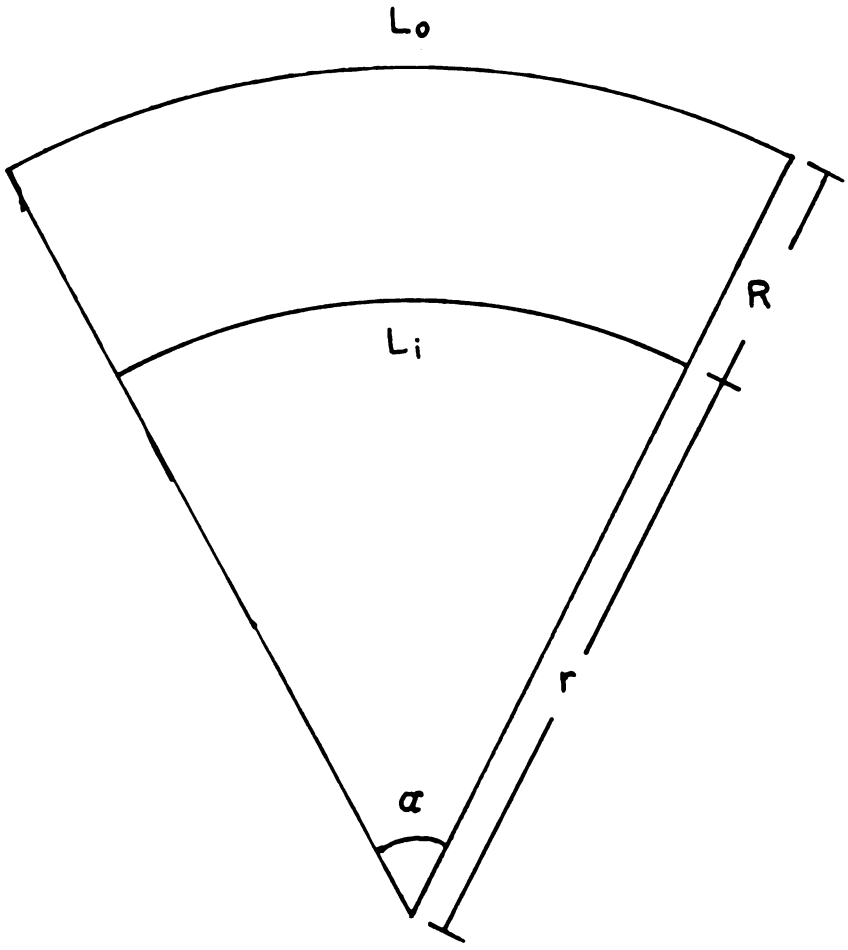

Figure 12. Template Parameters For Vanes

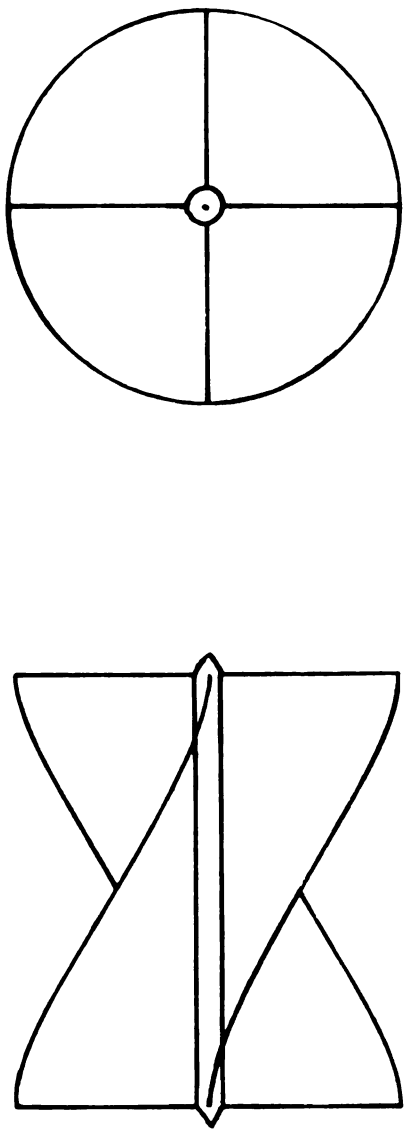

Figure 13. Assembled Vanes

6. Surface Barrier Detector

The detector used initially was a surface barrier type detector manufactured by ORTEC. This was a 2,000 μm deep detector with an active area of 160 mm^2. The device was operated at dry ice temperatures to improve resolution. This was done with a freon refrigeration system. The detector was mounted on a copper block, the interior of which was hollow to provide an expansion chamber for the refrigerant. (Figure 14) The block was electrically and thermally insulated from the spectrometer body by a nylon housing. The refrigerant feed-throughs were constructed from thin stainless steel tubing epoxied to the housing. A 500 $\mu m/cm^2$ Mylar window was used to protect the cold detector from condensates. The Marman flange connection was used to facilitate replacement of the surface-barrier detector by a Si(Li) detection system with a minimum amount of structural change. Relative efficiency (Figure 15) of the detector was measured with a thin, windowless ^{207}Bi source 2 cm from the detector face. The relative electron intensities are shown in Table 1.

7. Magnet Sweeping Electronics

A signal proportional to the magnetic field is taken from the Wavetec signal generator driving the Perkin current supply. The Wavetec signal is offset and amplified by a pair of operational amplifiers (Figure 16). The amplified signal is then fed to a voltage divider and adapter for the Perkin current supply. The signal is also fed to the internal potentiometer to provide a reference voltage for the SCA and the analog-to-digital converter (ADC), which monitors the spectrometer current. This whole circuit is wired into an overheat warning system such that when the magnet temperature exceeds 60°C, the reference voltages drop to zero,

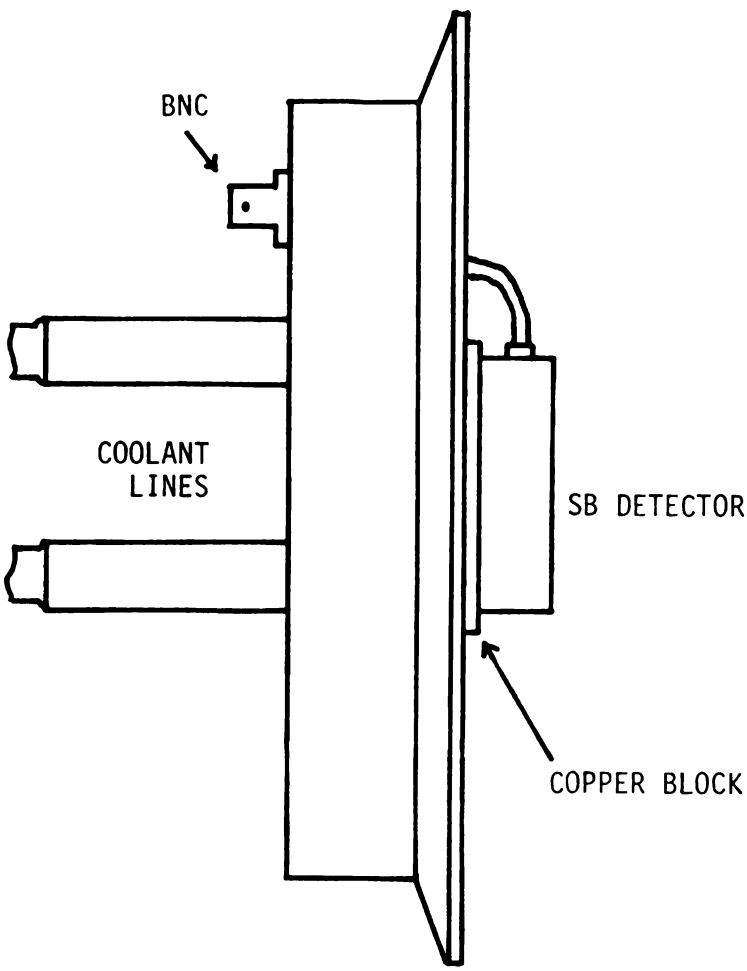

Figure 14. Surface Barrier Detector Mount

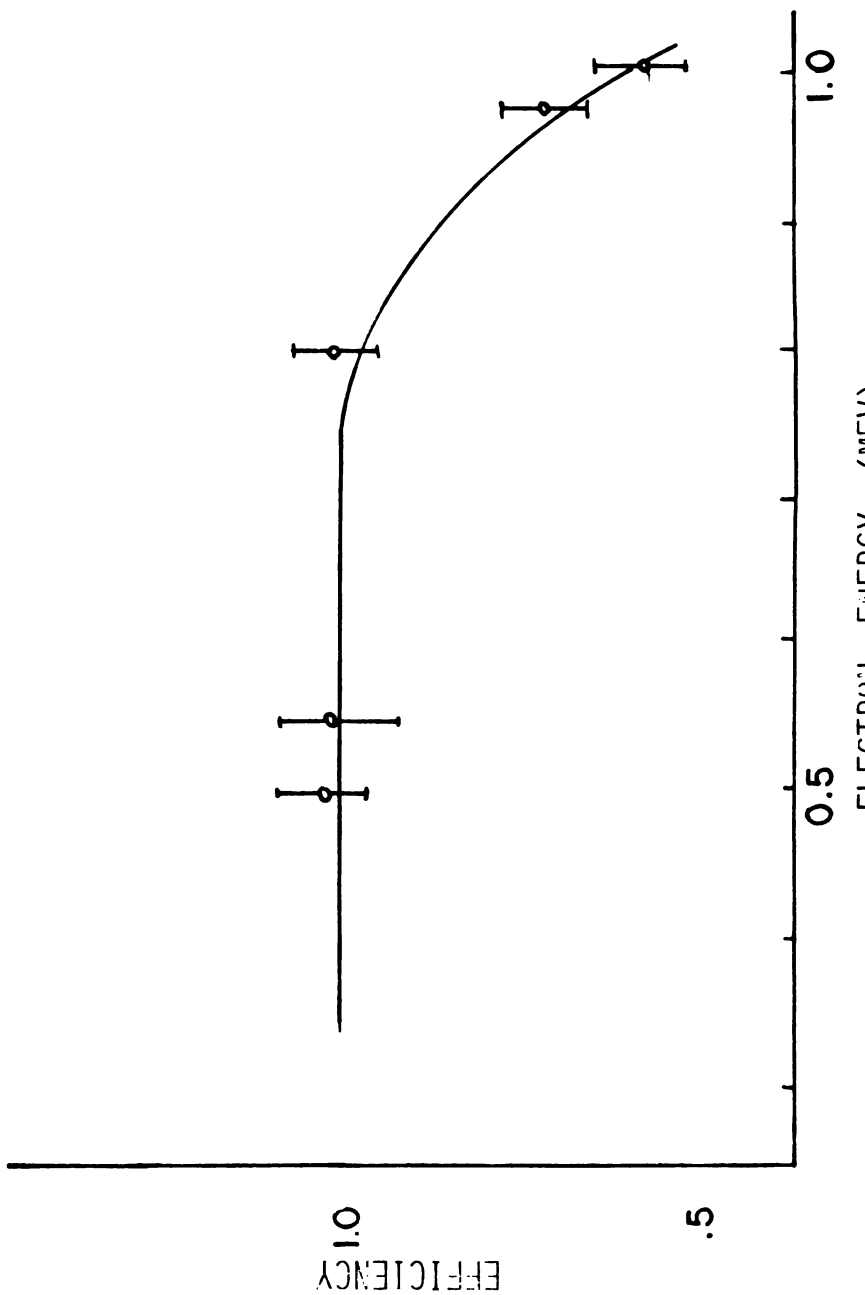

Figure 15. Relative Electron Efficiencies For Surface Barrier Detector

Table 1.

Relative Electron Intensities in ^{207}Bi from (Ha 68)

Transition Energy (keV)	Electron Energy (keV)	Transition Multipolarity	Electron Intensity
569.9	497.8	E2	1.7
	554.6	E2	0.35
	567.5	E2	0.16
1063.4	975.5	M4	8.2
	1047.6	M4	2.1
	1060.1	M4	0.72

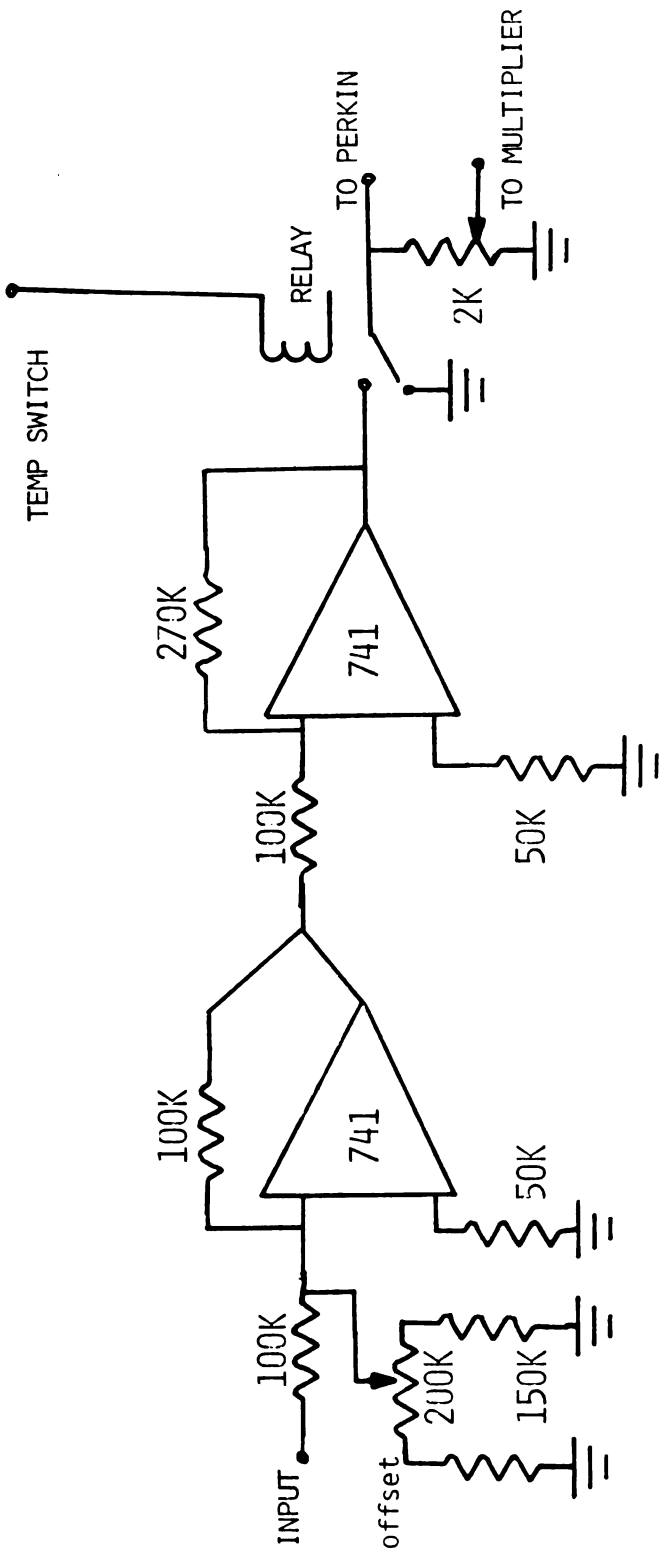

Figure 16. Magnet Control Electronics

shutting down the spectrometer.

Since the most effective detection of electrons is between the upper and lower transmission points of the spectrometer, and x-ray and gamma-ray detection is independent of the magnetic field strength, a method of sweeping a "window" with the field is desirable. This can be done with either a sweeping single channel analyzer (SSCA) or the program "TOOTSIE". (Ba 71)

8. "TOOTSIE"

"TOOTSIE" is a computer task used to classify 2-parameter coincidence data into one of up to 14 spectra using criteria determined by the user. (Ba 71) The program has the facility of allowing immediate plotting and data reduction.

During the "set-up" mode, the data are displayed on a storage scope in a 64 x 256 point matrix. With the spectrometer system, the matrix is divided into three regions, two of which contain unwanted counts, i.e., too high or too low to have passed through the magnet. The user determines these regions through a panel of switches mounted below a storage scope. The parameters used are energy and magnet current. Therefore, a region is defined which corresponds to the magnet momentum bite. This 64 x 256 matrix can be put on punched cards for contour or isometric plotting and analysis.

In the "run mode" coincidence data are stored in one of the three spectra corresponding to the regions defined by the experimenter.

9. Sweeping Single Channel Analyzer (SSCA)

An ORTEC 420A SSCA is used to determine the validity of the counts from the detector when "TOOTSIE" is not used. This device has the capability of using an external reference voltage in place of the lower level discriminator knob. The reference voltage, in this case, comes from the magnet sweep control which can be adjusted to match the amplifier gain. With this arrangement, only electrons in the proper energy range can pass through the vane system and be counted. Since x-rays and low energy gamma-rays are seen by the detector regardless of magnet setting, many of which lie outside the desired region defined in Section 8, their relative intensities will be reduced by this procedure.

10. Electronic Set-up

The signal from the detector is amplified and delayed before being sent to the analog-to-digital converter (ADC). The ADC receives a negative unipolar pulse which is stored by the computer. The prompt bipolar pulse from the spectroscopy amplifier is fed into a single channel analyzer which is swept in step with the magnetic field and used to provide a logic pulse for the gate and delay generators. With the program "TOOTSIE" two gate and delay generators are used to enable the ADC's. (Figure 17) The signal from the magnet sweep drive is squared by a multiplier and inverted by the operational amplifier to be fed into an ADC. Squaring the signal gives a linear relationship between magnet current and energy. Signals from the gamma detector were taken continuously.

When the SCA is used for gross momentum selection, the output of the operational amplifier is routed to the external lower level discriminator of the SCA. This enables the ADC only for the electron energies above

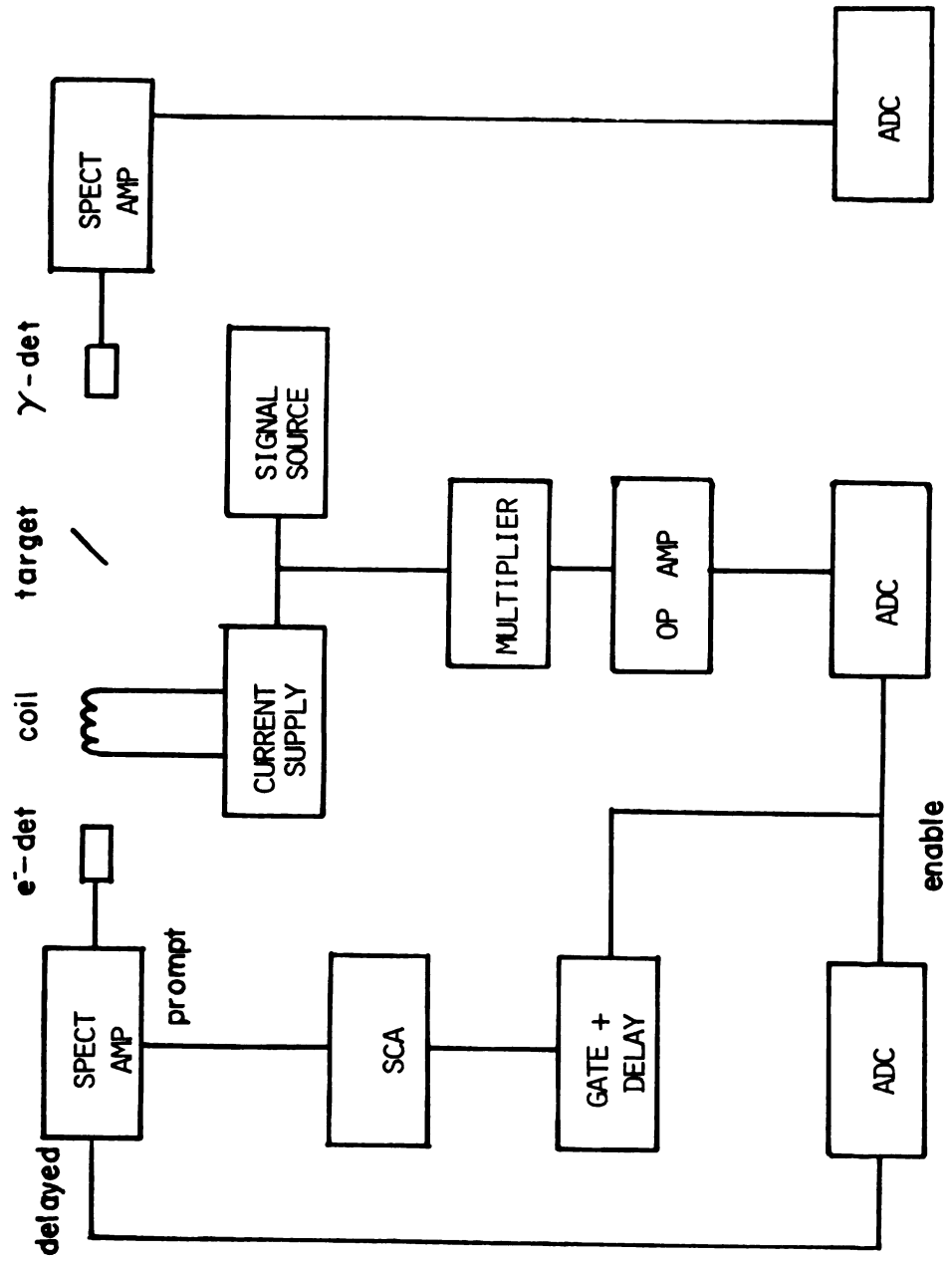

Figure 17. Electronic Set Up For Use With "TOOTSIE"

the spectrometer's lower threshold (Figure 18).

Briefly the procedure for setting up the spectrometer sweeping is as follows. Once the energy range of interest is determined, the magnet current range is taken from data presented in the testing section of this thesis. The offset of the operational amplifier is adjusted so that the output remains positive. This can be done with the signal generator set at audio frequencies on an oscilloscope. The output of the ADC is adjusted so that it stays above -6V DC (i.e., $|V_e| \leq 6$). Once this is adjusted, it can be connected to the ADC. Then, with the signal generator set at the sweep period, ~100 seconds, the magnet current range is adjusted to the value determined above.

A more complete description of this procedure can be found in the Appendix.

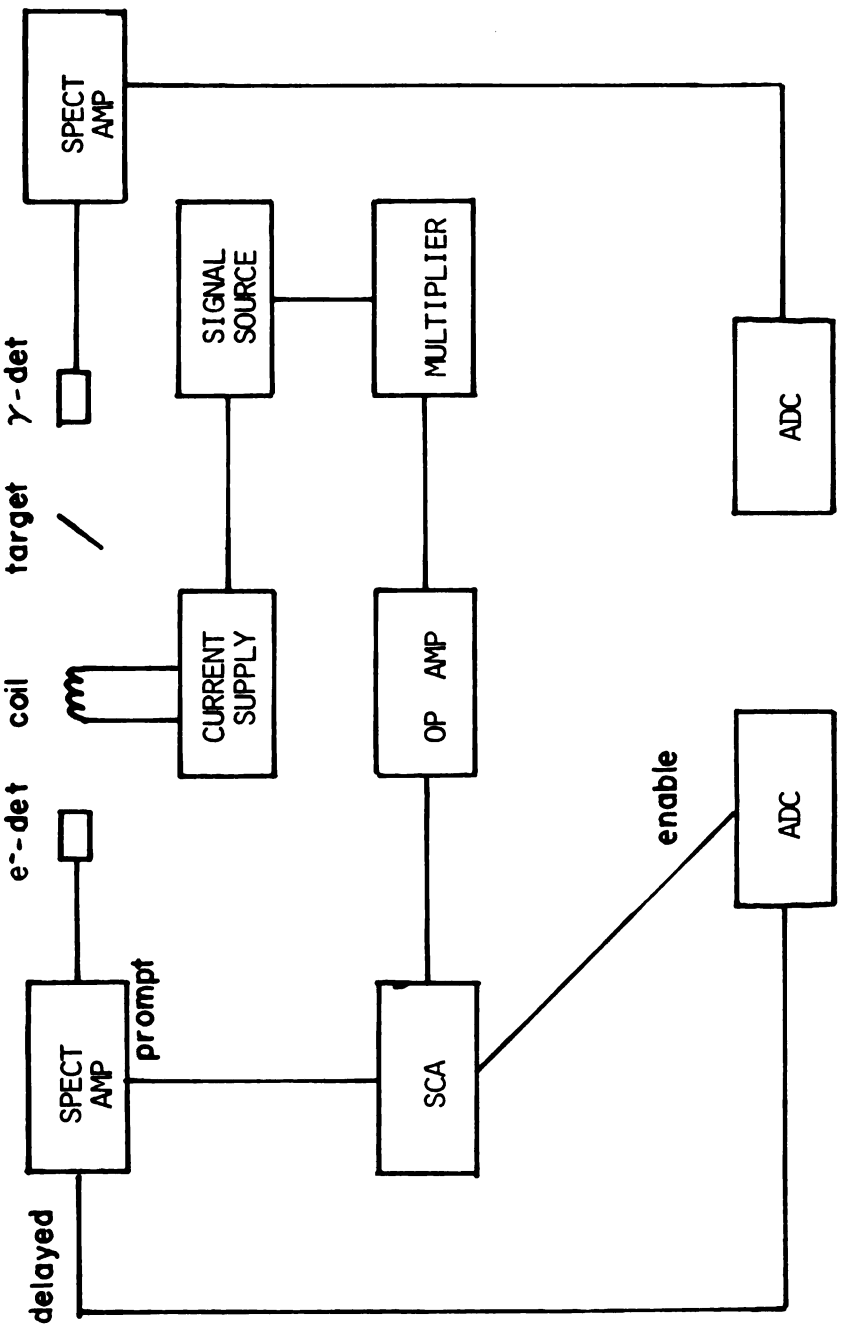

Figure 18. Electronic Set Up For Use With SSCA

TESTING

1. ^{207}Bi Source Off-Line

With the vanes in place, the system was tested for transmission with a ^{207}Bi conversion electron source. An offset sine wave was used for the sweep. This allowed an enhancement of both the high and low energy peaks. The spectrometer was set to sweep from 0 to 100 amperes. "TOOTSIE" was used to take data in a 2-D mode. In this mode the ordinate represents electron energy and the abscissa represents spectrometer current. Each point in this matrix contains the number of counts for a particular energy and current setting, therefore, a contour map of this matrix would tend to show the functional relationship of magnet current and electron energy. This can be seen in Figure 19. At a particular energy the contours show the coil transmission at each current setting. These are plotted in Figure 20 for the ^{207}Bi peaks. It can be seen that as the energy increases, the transmission width also increases. In Figure 21 the maxima of these curves is plotted (solid line) to show the relationship between magnet current and electron energy more clearly. The upper and lower transmission points are shown by the dotted lines. This resultant graph can be used to determine the current range needed to see a particular transition. The spectrometer current is determined by a shunt and digital voltmeter mounted on the cyclotron control panel. A reading of 10 mV corresponds to 50 amperes. For this reason magnet current is labeled in mV in Figure 21. This figure resembles Figure 19 in that if the counts in the contour map that lie between the dotted curves

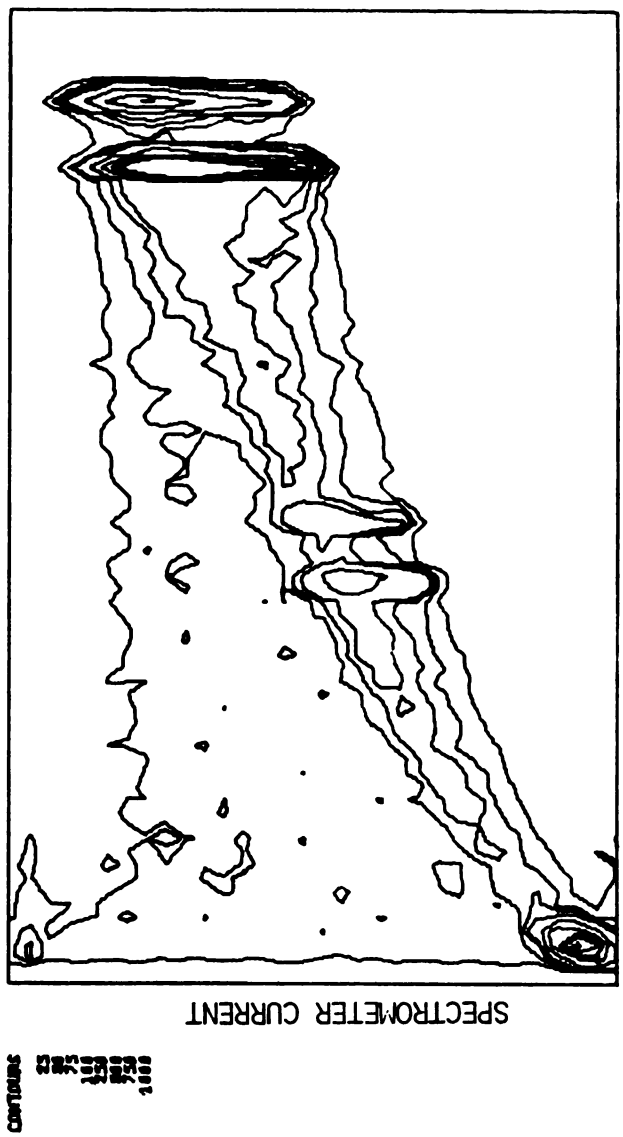

Figure 19. Contour Plot Of "TOOTSIE" Data (2-D Mode)

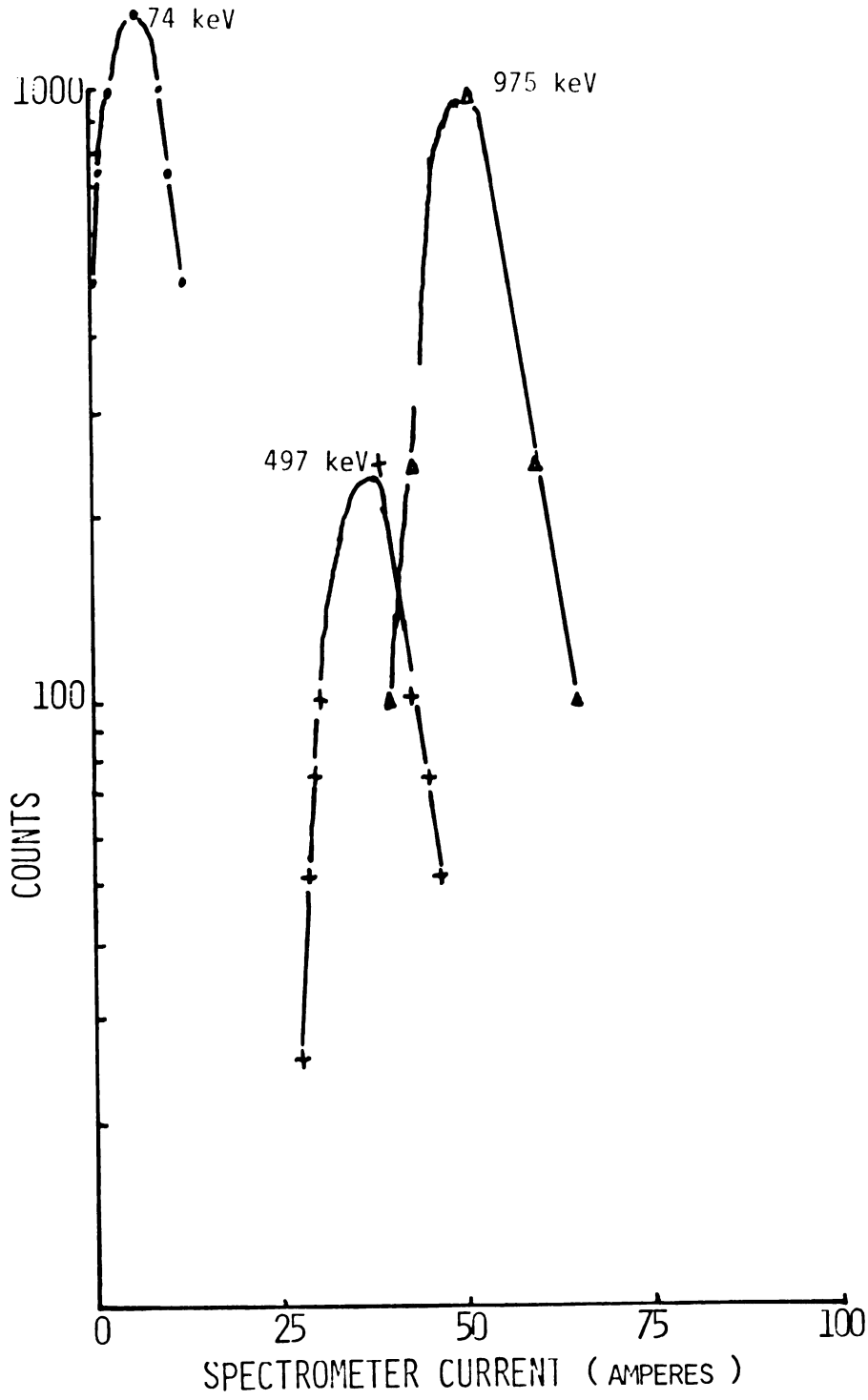

Figure 20. Magnet Transmission As A Function Of Spectrometer Current For Selected Energies

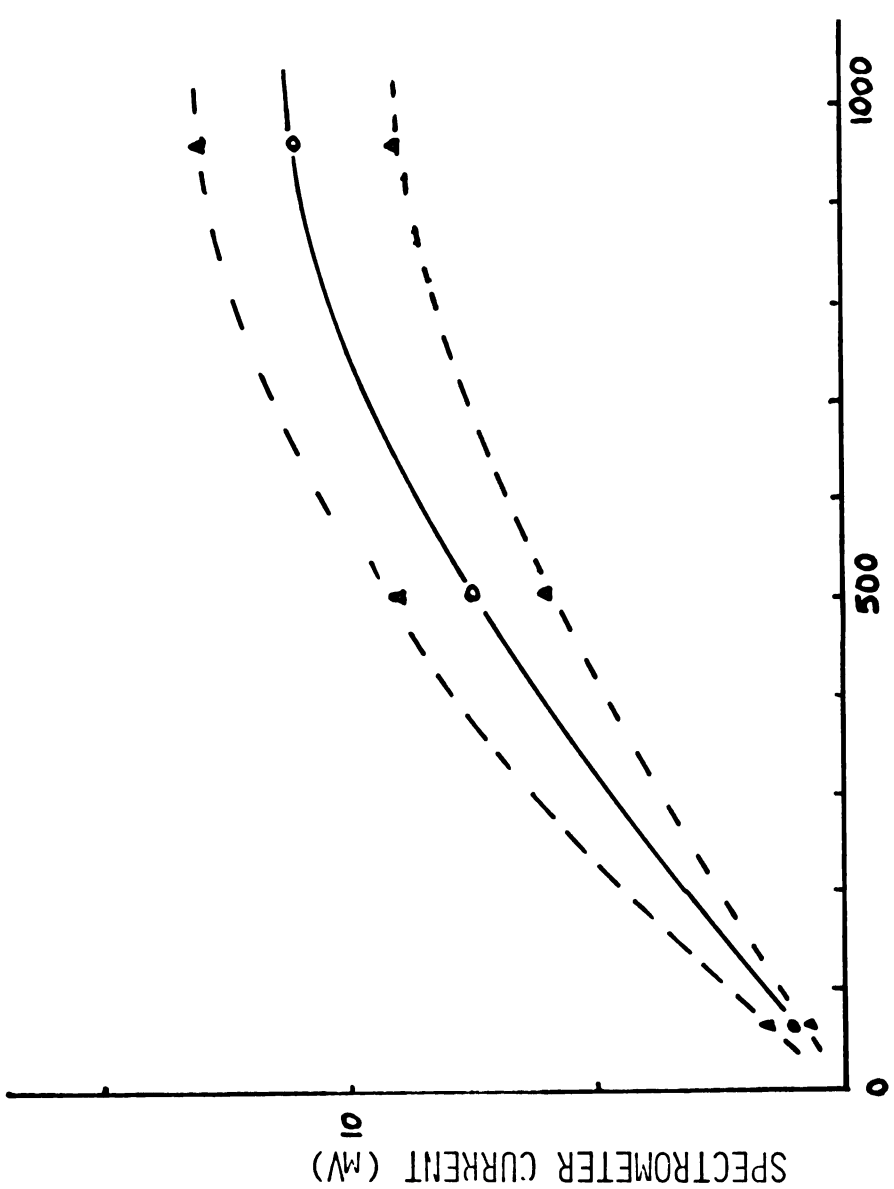

Figure 21. Spectrometer Window As A Function Of Current And Energy

in Figure 21 were plotted with respect to energy, a spectrum would result. Figure 22 shows such a spectrum. In this case "TOOTSIE" was used to determine the upper and lower curves. When designing an experiment, Figure 21 is used to determine the sweep range of the spectrometer current for the energy region of interest.

2. In-beam Reaction $^{154}Sm(\alpha, 4n\gamma)^{154}Gd$

To test the spectrometer in-beam, it was decided that the conversion electron spectrum of ^{154}Gd would be studied. This experiment was performed by Gono and Sugihara (Go 74) at Texas A & M and provided us the data to check our results.

The level scheme of ^{154}Gd developed by Khoo, et. al., (Kh 73), shows a ground band and ß-vibrational band established to $J^{\pi} = 18^{+}$. (Figure 23) In the past, spin assignments for most states studied by on-line gamma-ray spectroscopy have been made on the basis of gamma angular distribution measurements. However, in the case of long lived states, such as some three and four quasiparticle isomers in deformed nuclei being studied here, this method is not acceptable, because the isomeric transitions display isotropic angular distributions. Even in cases where strong anisotropies exist, unambiguous J^{π} assignments frequently cannot be made, and systematic or model dependent features are often relied upon for assignments which are experimental. In these cases, internal conversion coefficient measurements can be used to help determine the multipolarity of the transitions.

The cross section for an (alpha, xnγ) reaction on ^{154}Sm is shown in Figure 24. A beam energy was chosen to be 48 MeV in order for the $(\alpha, 4n\gamma)$ reaction to dominate and feed levels in ^{154}Gd.

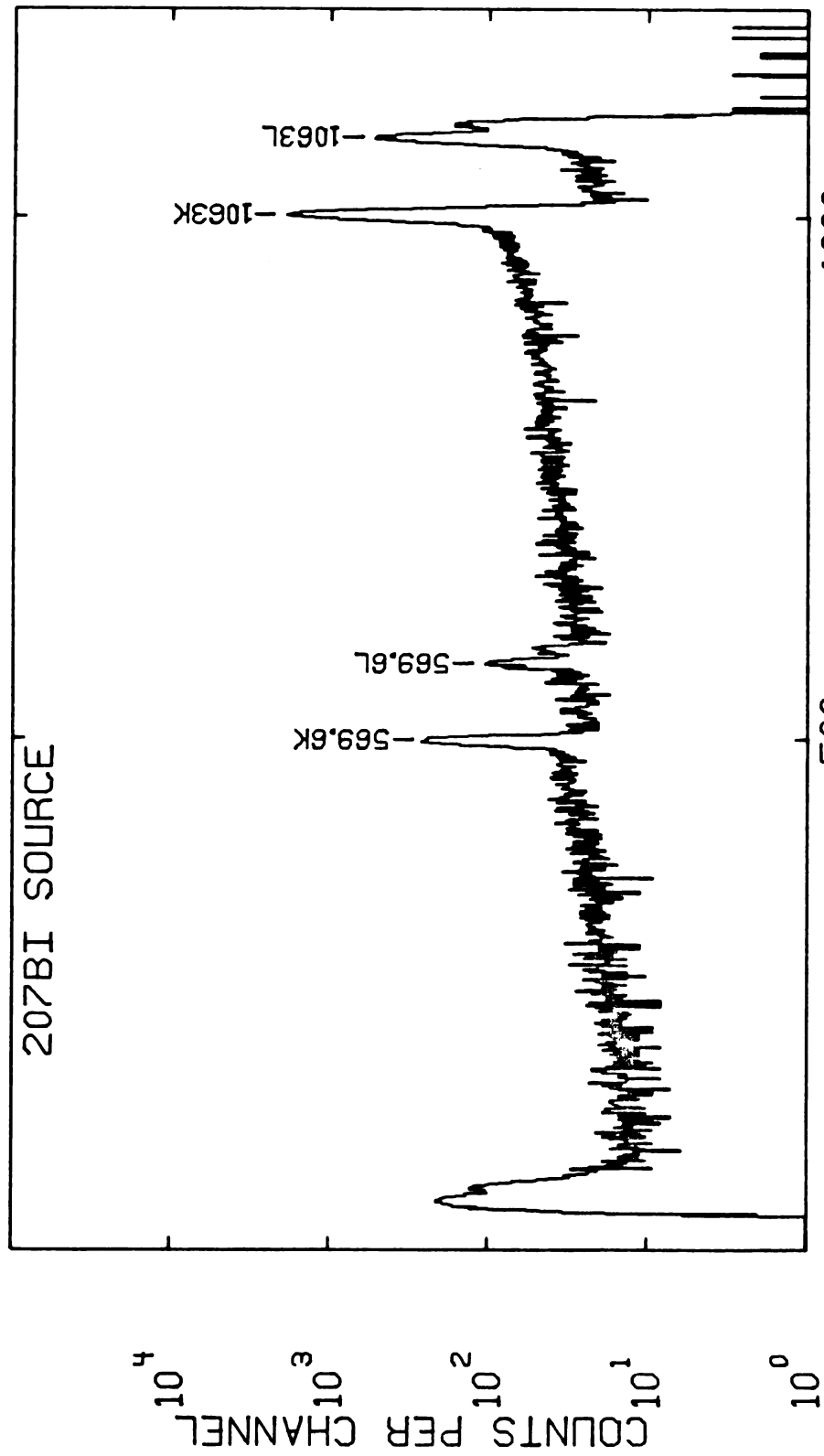

Figure 22. ^{207}Bi Electron Spectrum As Taken By "TOOTSIE" (Run Mode)

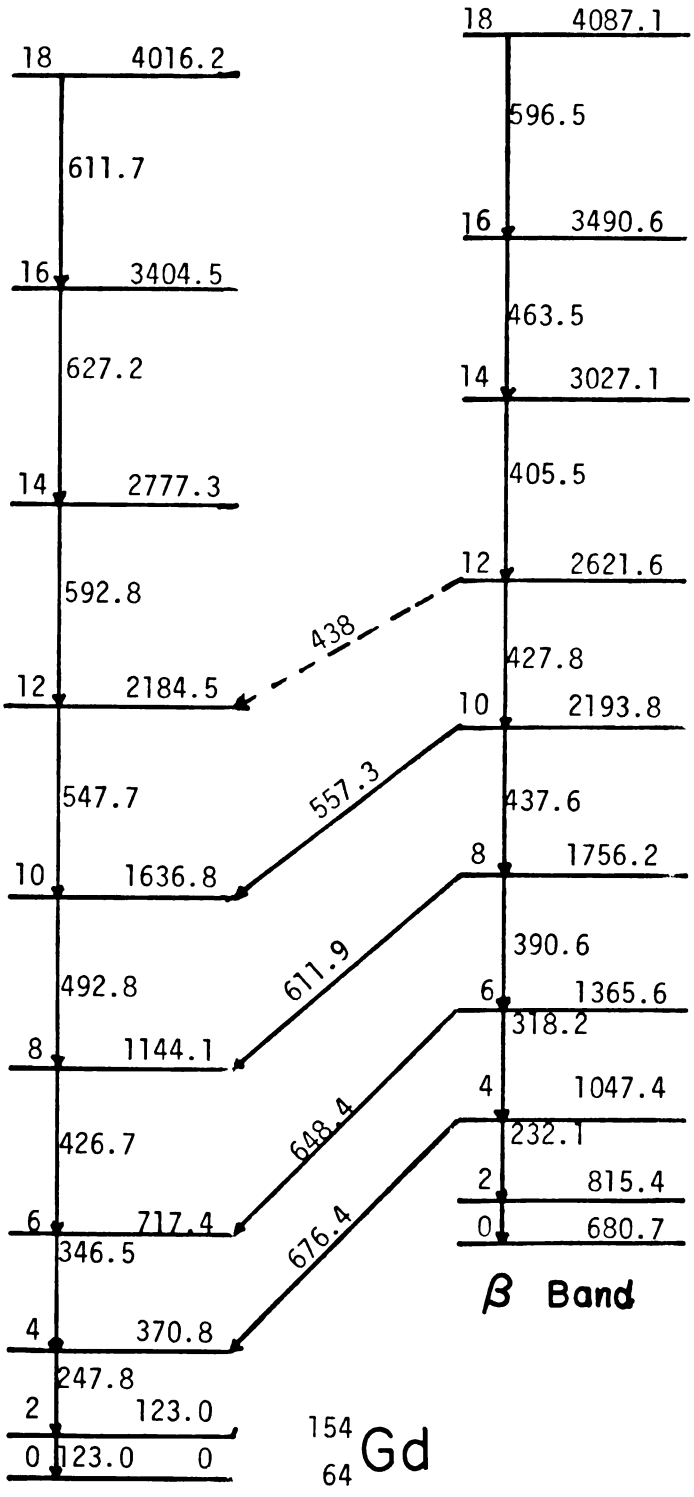

Figure 23. Level Schemes Established By Khoo, et.al. (Kh 73)

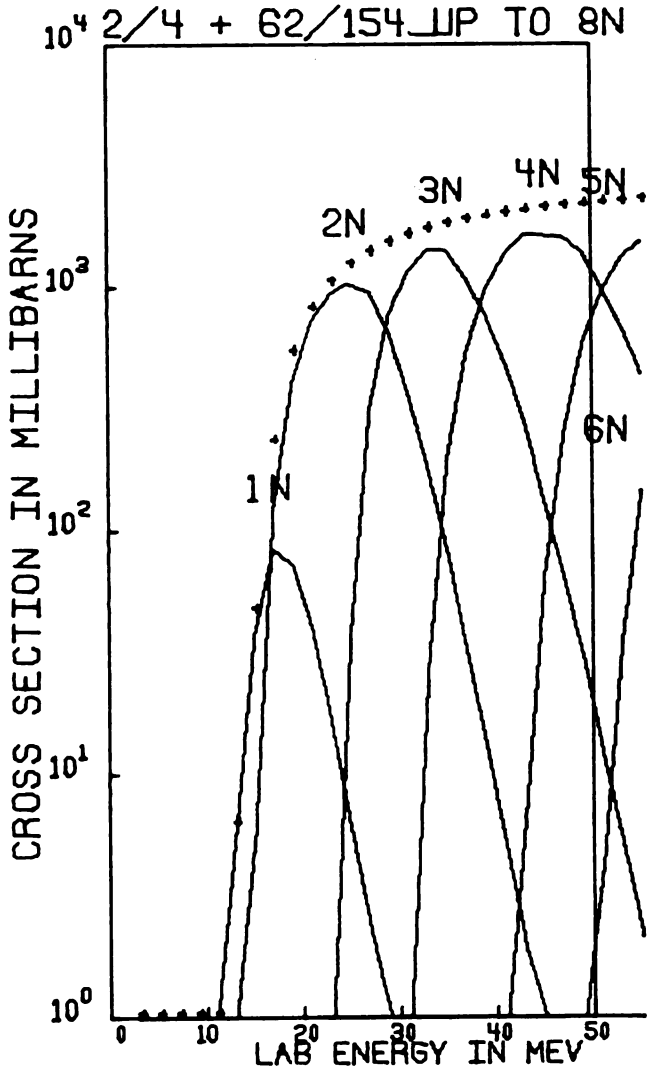

Figure 24. Reaction Cross Section For (α, nxγ) Reaction On ^{154}Sm

3. Target Preparation

To prevent loss of resolution of the conversion electrons, thin targets must be used. 17.00 mg of Sm_2O_3 (154 isotope enriched) was combined with fine zirconium powder (220 mesh) and water to make a paste. The zirconium was used for the reduction of the samarium at low temperatures. After drying, this mixture was placed in a zirconium tube with a #72 hole. This was clamped into the evaporation apparatus.

The target frame was prepared by mounting two layers of Formvar ($5\mu g/cm^2$), over a 19 mm hole and depositing 20 $\mu g/cm^2$ of carbon onto the Formvar. A 13 mm mask and a 4 mm heatshield, both of tantalum, were mounted over the zirconium boat.

A current of 170 amperes was passed through the boat for a short time to out-gas the paste. The target was then moved in and the reduction and evaporation of the ^{154}Sm allowed to continue. The result was a nice uniform target trying to curl at the edges. The thickness was measured to be 550 $\mu g/cm^2$. The target was then stored under vacuum until needed. A more complete description is given by Nolen, et. al. (No 73)

4. On-line Results

An electron spectrum (Figure 25), was taken for 45 minutes with a beam current of 15 nA. The alpha particle energy was 48 MeV. Of particular interest in the experiment was the effect of the vanes on positron reduction and the focusing effect of the magnet. It was found that the peak-to-background ratio was good, (37:1 for the 352 keV transition), indicating that the discriminator settings from "TOOTSIE" were correct. The effect of the vanes on positron reduction was tested by reversing the current leads to the spectrometer and noting the relative count rates on

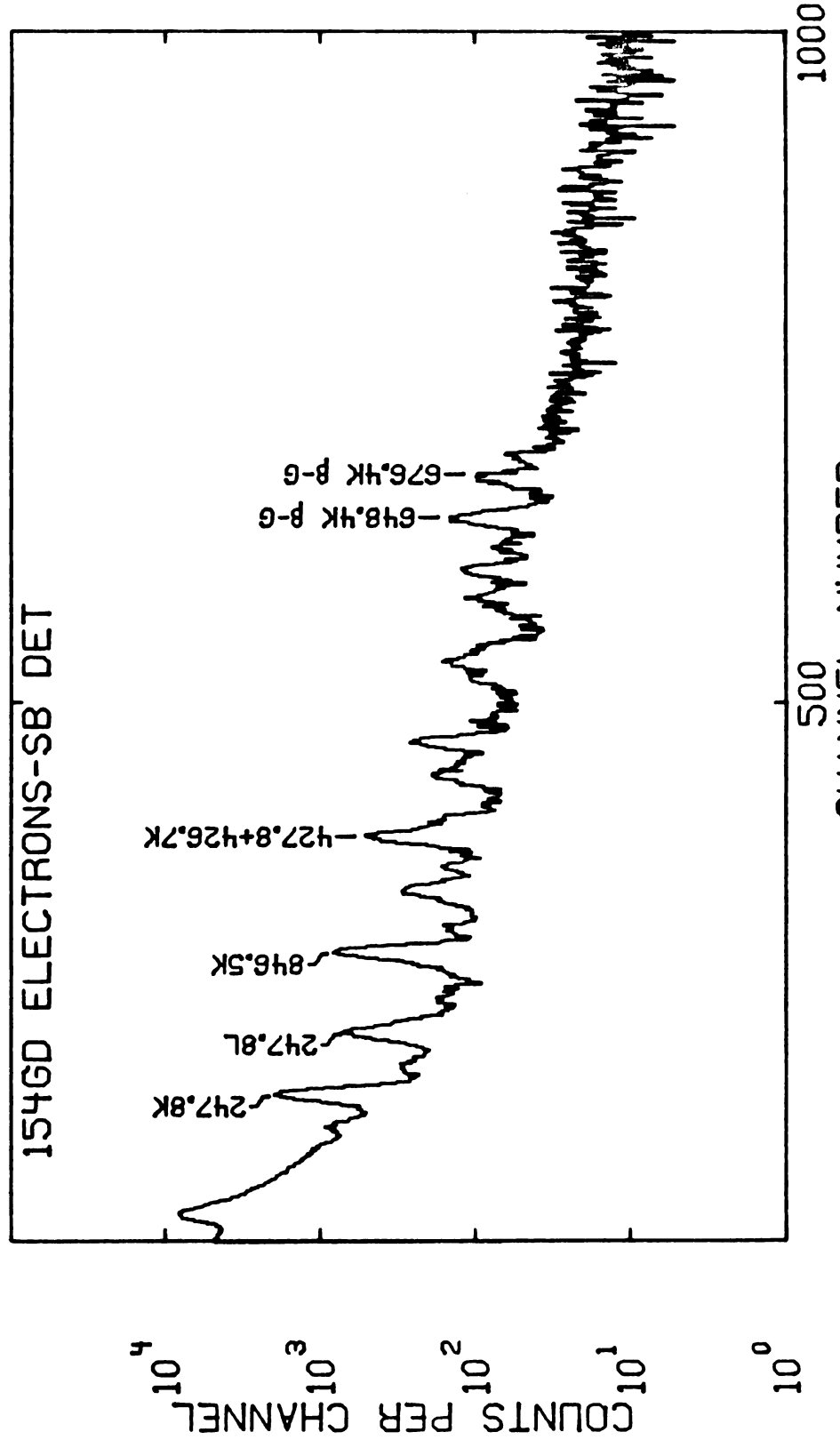

Figure 25. In-beam Spectrum Of ^{154}Gd

a rate meter. It was found that the ratio of electrons to positrons (reversed electrons) was approximately 1000:1. Once it was determined that the spectrometer was working properly, a high resolution Si(Li) detector was ordered to provide resolutions comparable to the Ge(Li) gamma-ray detectors.

Si(Li) DETECTOR

1. Mounting to the System

A high-resolution Si(Li) detector was purchased from KeVex Corporation. This detector is 3 mm deep with an active area of 80 mm^2. Resolution was warranted for 2.5 keV at 975 keV; 3.3 keV was measured with the source in air through a 500 $\mu g/cm^2$ window with the detector bias at 300 volts. The detector head assembly included a cooled FET and came with a matched charge sensitive preamp.

The head assembly was mounted on a 3/8 inch diameter cold finger and enclosed in a right-angle cryostat. A thin window of 1/4 mil Mylar was mounted on the face of the cryostat to allow transmission of low energy electrons with a minimum loss of resolution. The cryostat snout was made of aluminum with 4 mm wall thickness to minimize the mass of the medium surrounding the detector. (Figure 26)

The cryostat was connected to the system via a 2 inch gate valve and a sliding seal. This arrangement allows the experimenter to change targets or sources without breaking the thin Mylar window on the cryostat or warming the detector. Also, it allows for adjustment of the target-to-detector distance and for shielding the detector during beam alignment. Unfortunately, this thin Mylar window is not opaque to light and so some care must be exercised when the detector is biased.

The detector was tested for efficiency and resolution with a ^{152}Eu source. The spectrum (Figure 27), was analyzed and the resulting

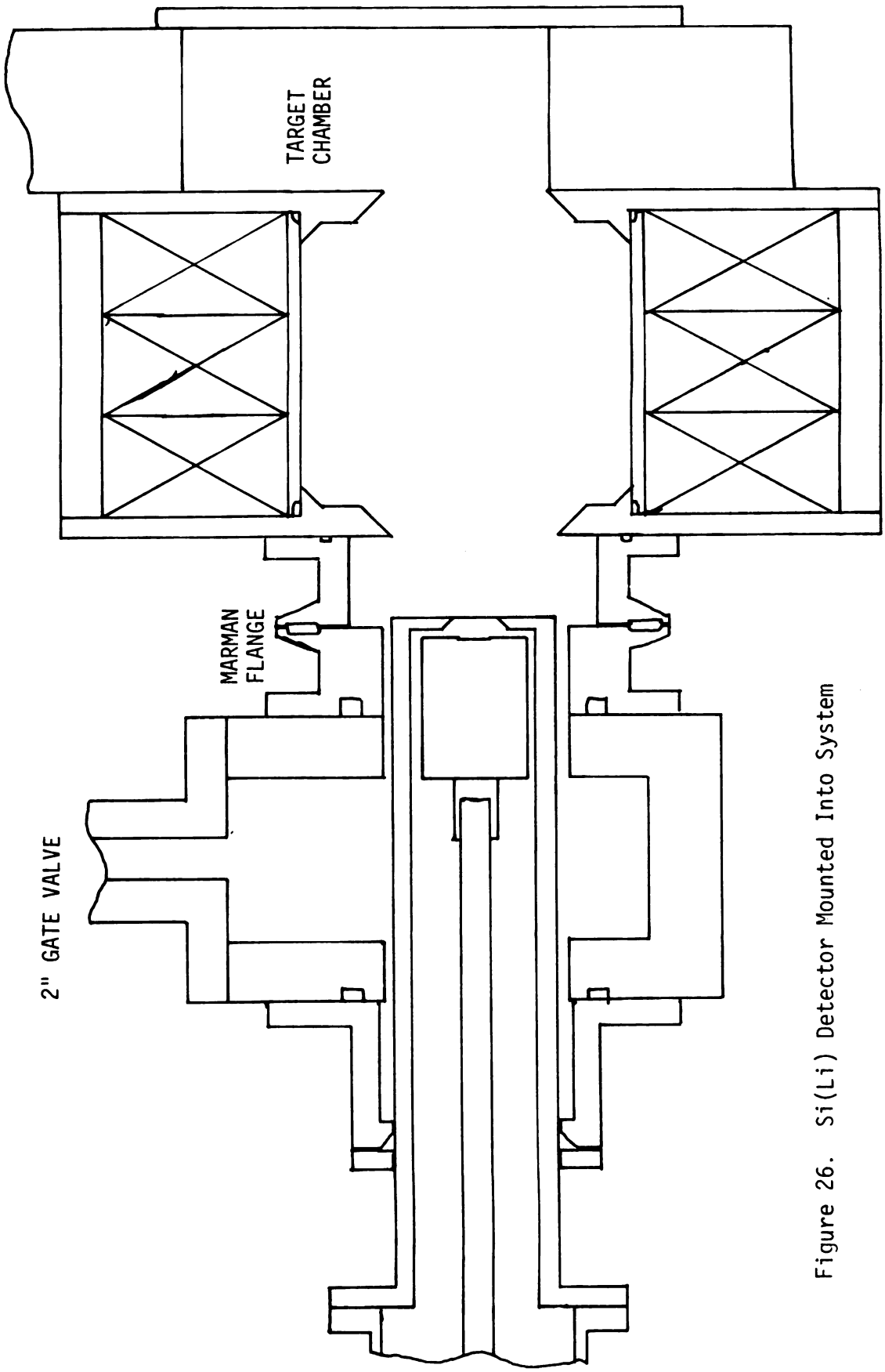

Figure 26. Si(Li) Detector Mounted Into System

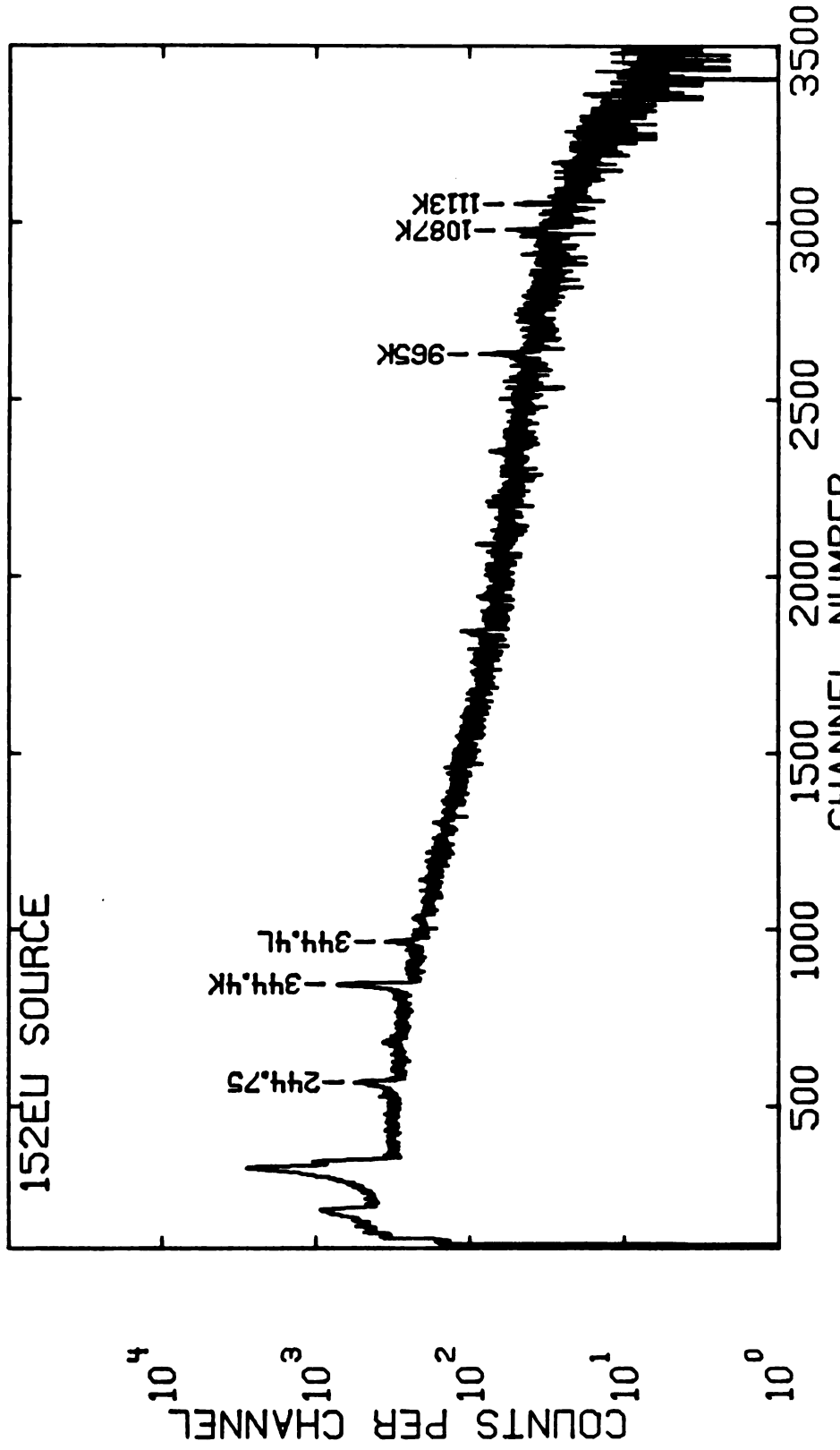

Figure 27. ^{152}Eu Efficiency Spectrum

efficiency plotted (Figure 28). The relative electron intensities are shown in Table 2.

2. On-line Tests

The Si(Li) detector was tested with the system. A ^{154}Sm (α, 4nγ) ^{154}Gd reaction was used again with an alpha energy of 50 MeV and a beam current of 30 nA. The spectrum shown in Figure 29 was taken over a period of one hour. The target thickness was 500 $\mu g/cm^2$. Two subsequent spectra were taken with the sweep turned off and the magnet current held constant. They are shown in Figure 30. Comparing these to the swept spectrum gives a visual representation of the momentum bite of the spectrometer. The ratio of these spectra to the swept spectrum is plotted in Figure 30 to show this momentum bite.

After the cyclotron was changed over to protons, three more targets of $^{116, 117, 118}Sn$ were bombarded with 8 nA of 10 MeV protons for five hours each. The typical reaction was $^{116}Sn(p, n\gamma)^{116}Sb$. The ^{116}Sb spectrum (Figure 31) exhibited a large broadening of the electron peaks. This was due to the thickness of the tin target which was 11.5 mg/cm^2. The ^{117}Sb (Figure 32) and the ^{118}Sb (Figure 33) did not show this broadening because of their relative thinness (2.6 and 1.8 mg/cm^2 respectively). Of particular interest in the ^{118}Sb spectrum were conversions of suspected low lying level transitions in the range of 20-70 keV. These were not observed in these runs due to a high LLD setting on the SCA. It may be possible to overcome this problem with a higher gain and lower magnet current setting.

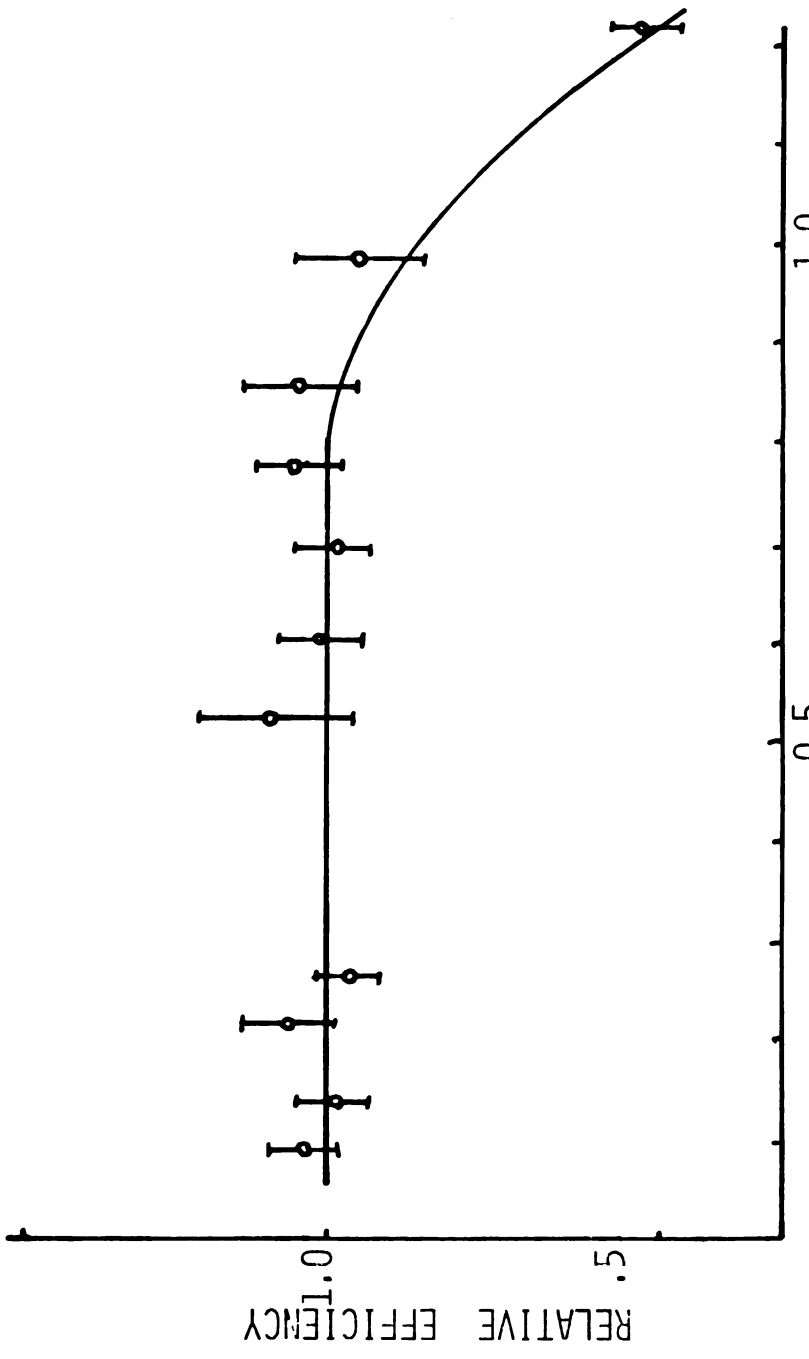

Figure 28. Relative Efficiency For Si(Li) Detector

Table 2.

Relative Electron Intensities For ^{152}Eu (Wy 71)

Electron Energy (keV)	Relative Intensity
198	82.0
237	27.0
294	100.0
336	26.0
360	5.9
395	3.1
531	1.4
564	0.9
609	0.9
641	3.6
725	2.9
815	1.6
916	4.4
955	1.1
1032	2.9
1056	3.0
1362	1.4

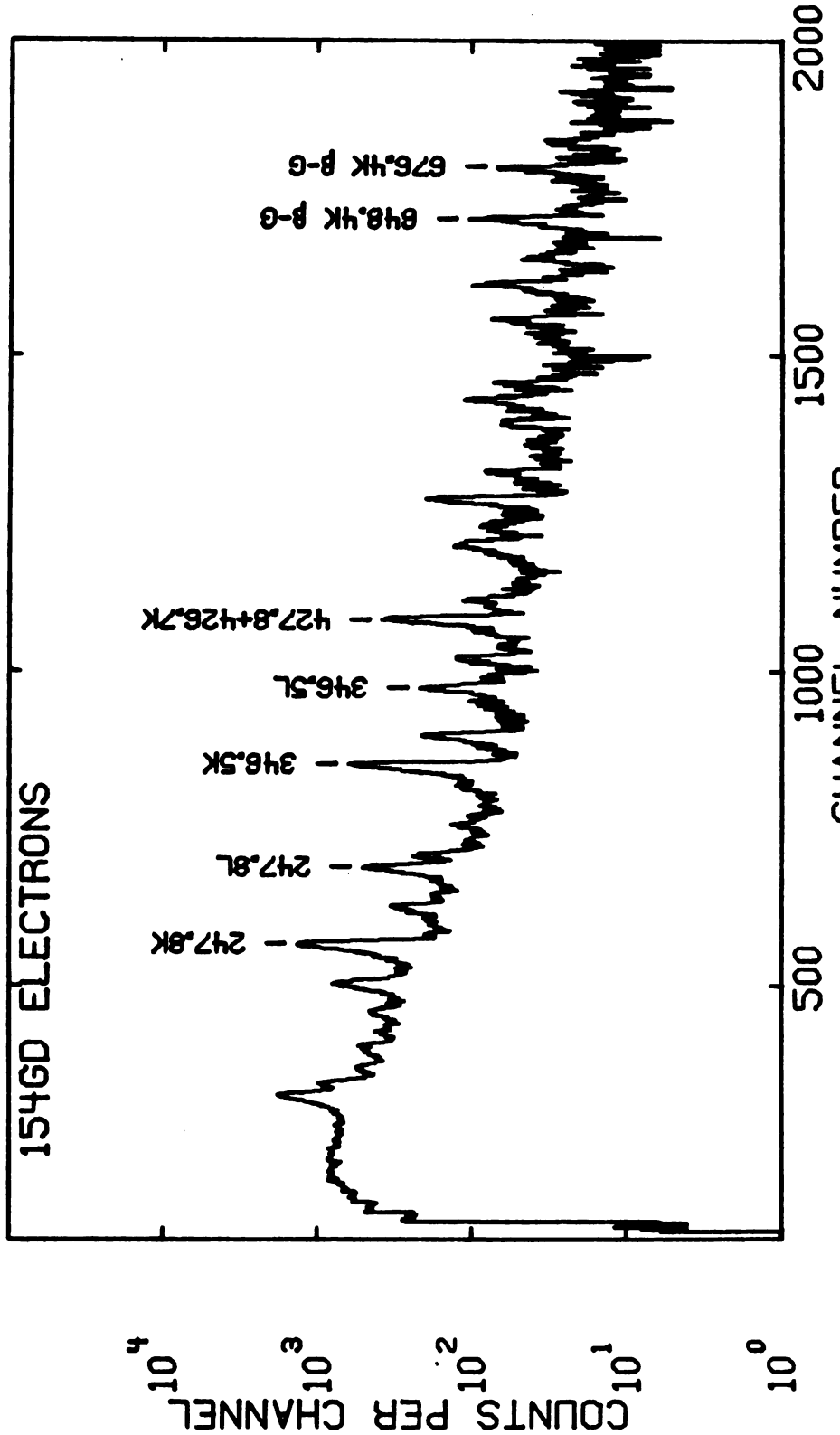

Figure 29. ^{154}Gd Spectrum

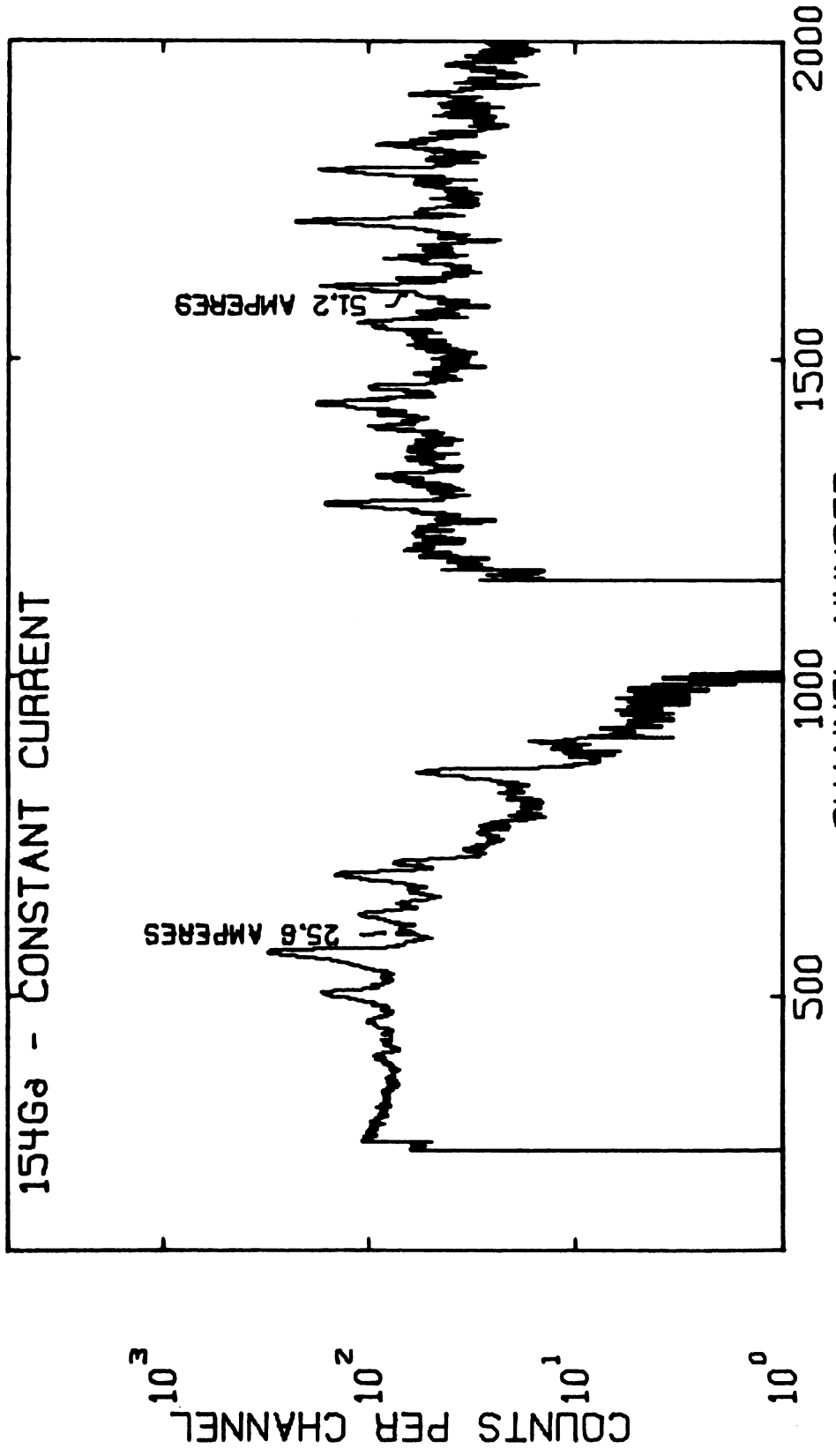

Figure 30. Constant Current Settings To Determine Window Width

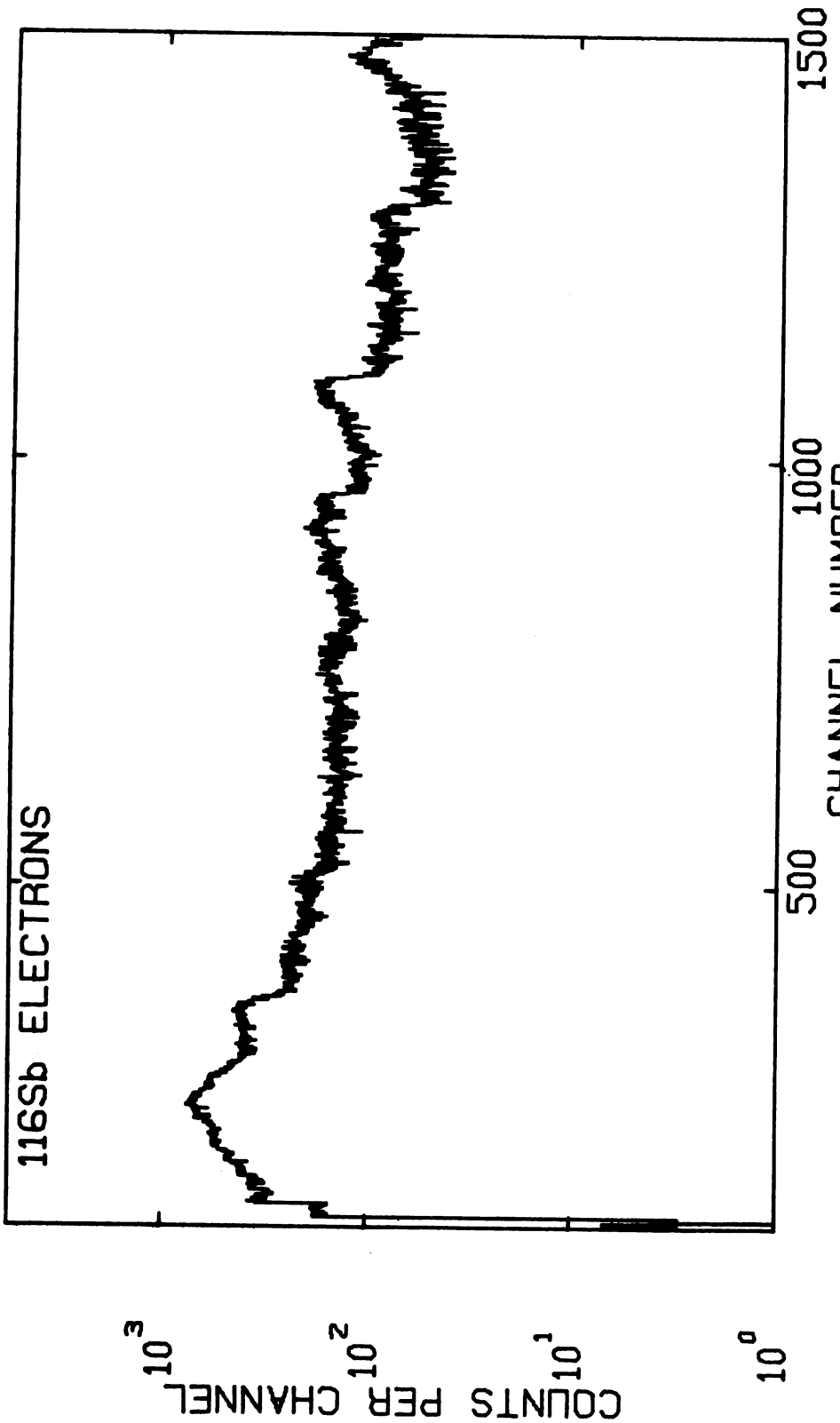

Figure 31. ^{116}Sb Spectrum

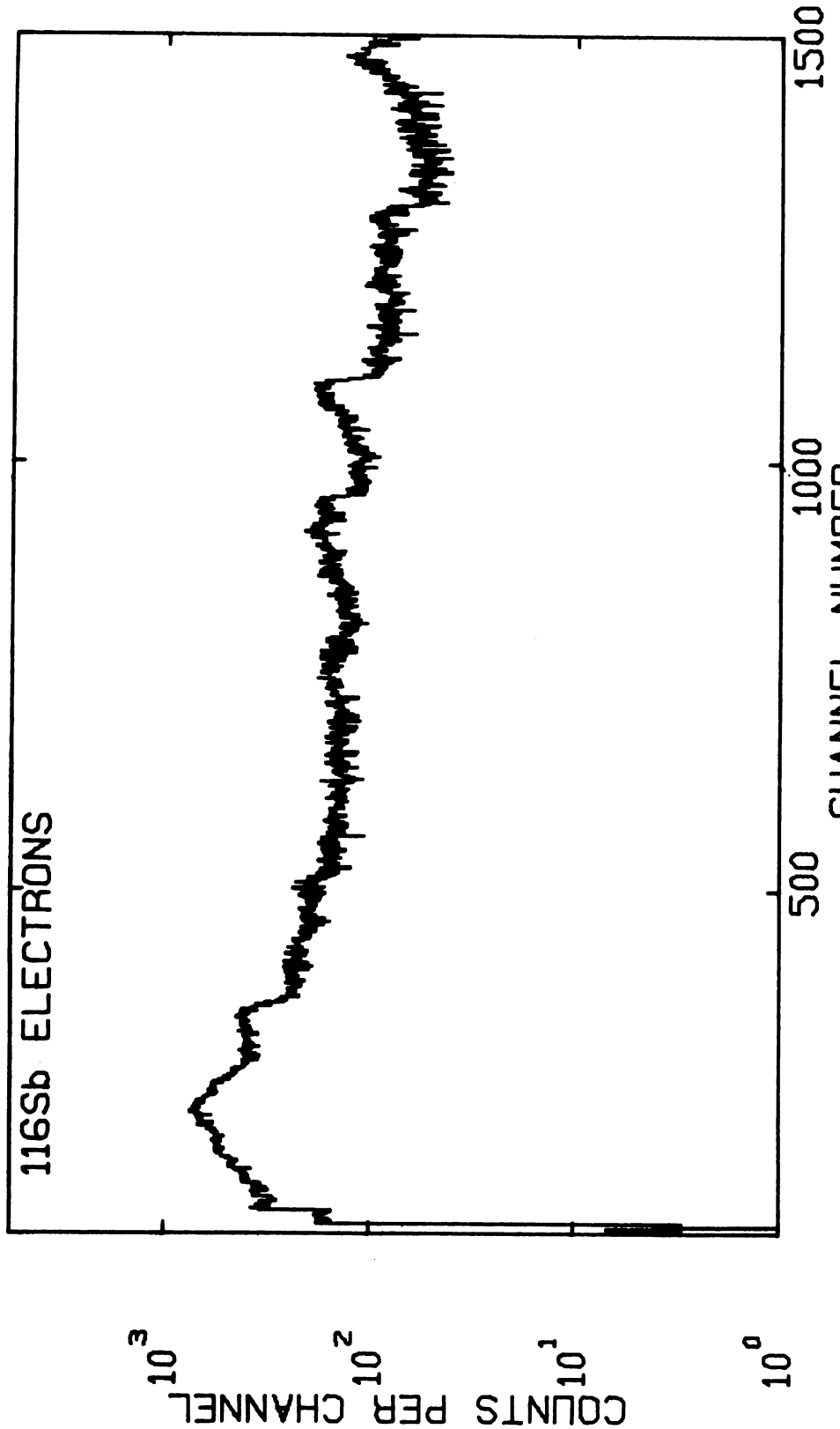

Figure 31. ^{116}Sb Spectrum

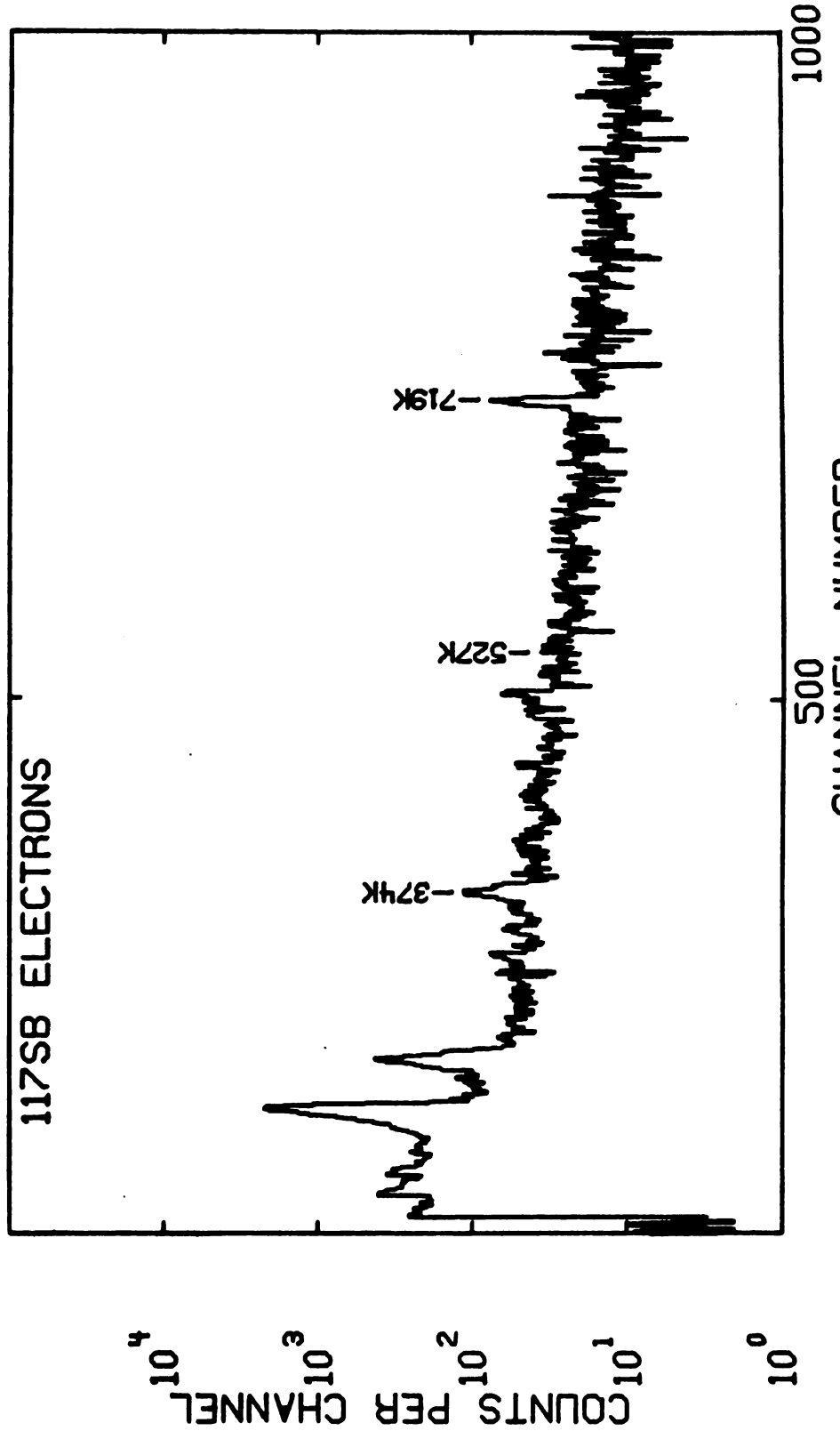

Figure 32. ^{117}Sb Spectrum

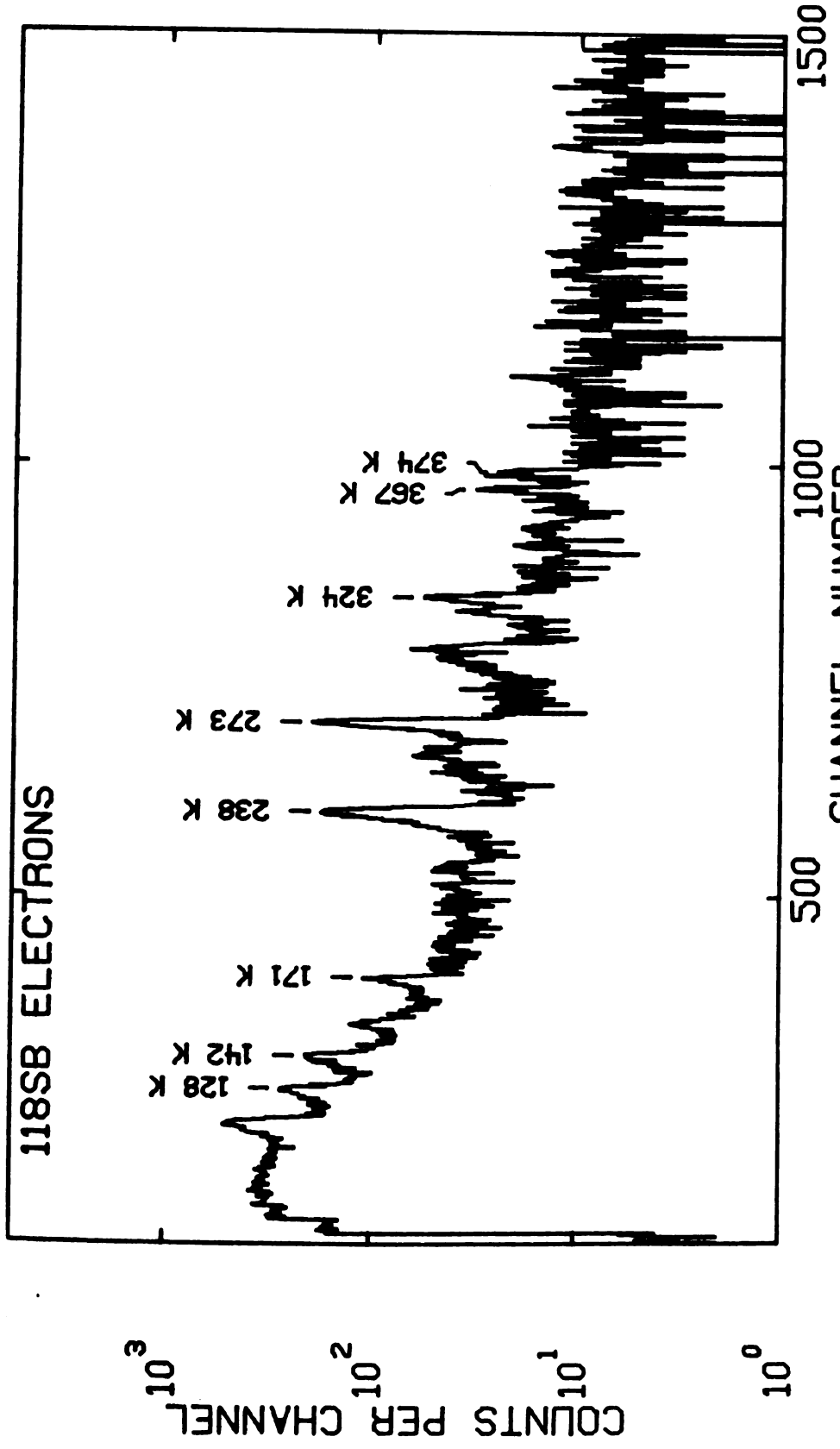

Figure 33. ^{118}Sb Spectrum

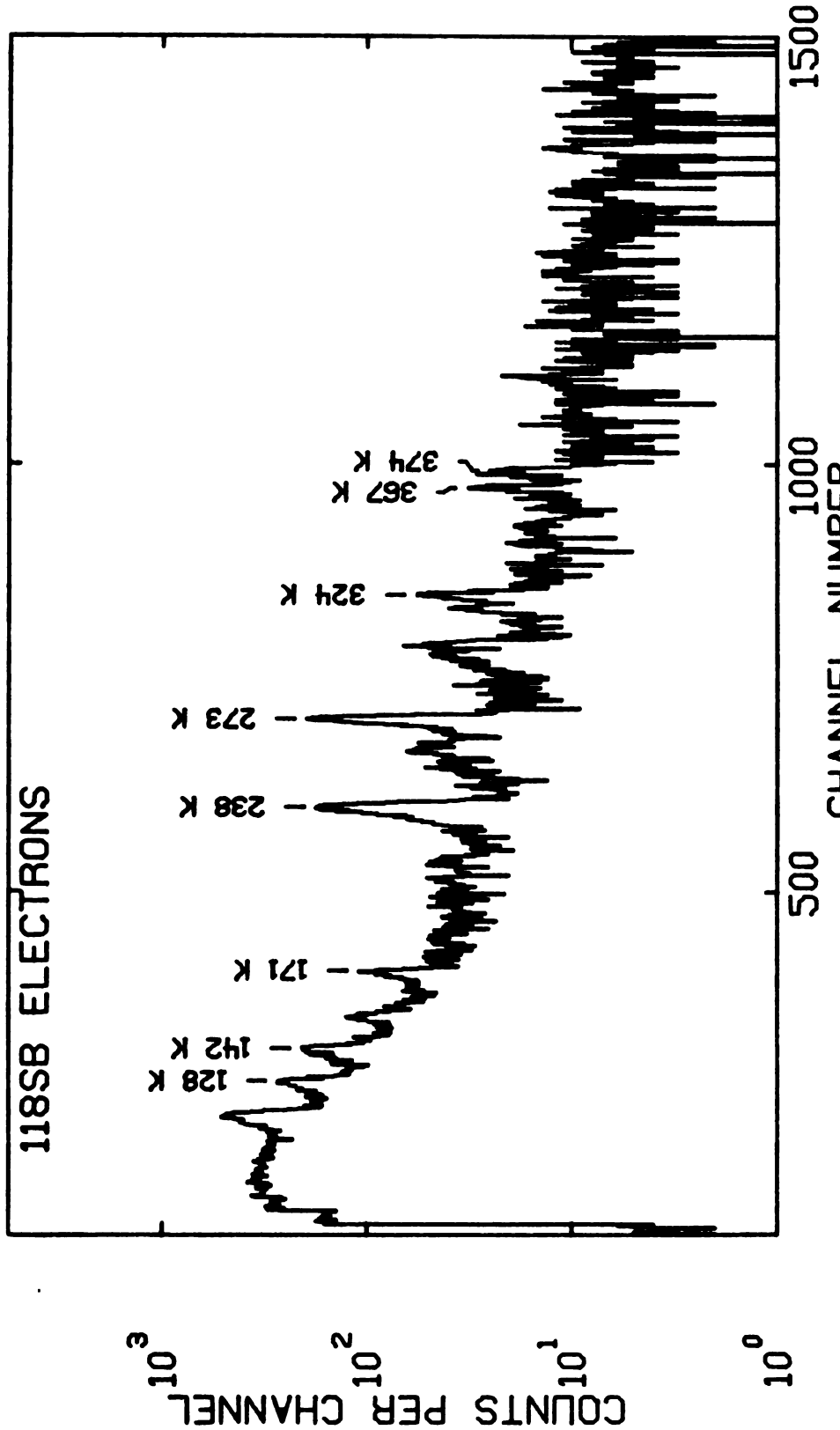

Figure 33. ^{118}Sb Spectrum

CONCLUSION

The conversion electron spectrometer tests have shown that the device can be used to acquire electron spectra in-beam. The large acceptance angle insures a high count rate and transmission of electrons beyond the effective energy range of the Si(Li) detector (2 MeV). The anti-positron vanes and center plug are effective in both the stopping of positrons and x-rays and defining the electron energies that pass through the coil. This reduces the high background count rate due to ionization electrons and positrons. By using a high resolution detector for energy determination, higher count rates and shorter data collection times can be obtained over those obtained from an "orange" or single energy spectrometer. The modular design of this spectrometer gives an experimenter great freedom in experimental design, allowing variability of energy range, target site and choice of detector.

Due to the Si(Li) detector's relatively high efficiency for x-rays, low energy conversion electron peaks are sometimes masked by x-ray peaks in a spectrum. Although these x-rays are attenuated by the sweeping window and lead center plug, they may continue to be a problem in future experiments involving nuclei with low lying states because of fluoresced x-rays from the lead itself.

Another problem that has arisen is the variability of the incident beam intensity. Because the electron energy range is swept, a short period of low or high beam intensity will raise or lower the peak height

in the area where the spectrometer current was set during the beam intensity variation. This problem can be partially solved by making more sweeps with the spectrometer thereby averaging the loss of counts.

The spectrometer has shown that it can be used to take high resolution electron spectra and that the sources of error discussed can be remedied by careful experiment design.

APPENDIX

APPENDIX

Using the Conversion Electron Spectrometer

In using this device, one must keep in mind that conversion coefficients are often quite small and that electrons, in passing through matter, lose energy quite easily. The former point leads to low counting rates. The second point forces the experimenter to use only thin targets in order to achieve the low resolution needed in order to accurately determine the conversion coefficients. One should then expect low electron count rates.

1. Mounting the Device

The spectrometer mounts on the existing coincidence chamber, so it must be mounted on the beam-line. Since a good vacuum insures a long electron free path, it is recommended that the diffusion pump be used with this set-up. A beam-line tee fitting is available for this purpose. When mounting the coincidence chamber, be sure that the extension to the chamber is attached so that there will be clearance for the magnet. One of the windows is replaced by the aluminum adapter and the magnet is bolted to the chamber.

The cooling water connections are made before the current leads are attached. The black lead (+) is connected to the black clamp that is the nearest to the perimeter of the coil. This polarity insures that electrons will pass through the spectrometer when the console digital voltmeter reads negative. A conversion electron source is then placed in

the target position. This source should be windowless and as thin as possible in order that the resolution of the conversion electron is preserved. The beam-line is then pumped down. Once the roughing is completed and the diffusion pump is working, the valve protecting the detector can be opened and the detector slid into place. This should be done slowly so that the detector is not jarred. The detector has a nylon cover on its end to stop the detector at the correct position. With a Simpson meter, check the detector cryostat to see that it is not in electrical contact with the beam-line. Any contact is undesirable since it would cause ground loop noise in the electronics and consequently decrease resolution. Check to see that the vacuum is holding and start connecting the electronics.

2. Electronics

The output of the electron detector and supporting electronics can be tested like any of the Ge(Li) detectors that are now in use. However, a 100 keV electron has a velocity of 0.3c and it must travel 10 cm to the detector. The time for the electron to pass through the magnet is on the order of 10 nano-seconds. Although this time decreases quickly with increasing energy, this could be a problem to be considered in coincidence experiments.

In order to reduce unwanted counts (i.e., too low in energy to have passed through the magnet correctly), a sampling of the magnet current is taken so that count/no count decisions can be made either through hardware (Sweeping Single Channel Analyzer) or a computer program. At any rate, one should collect the following electronic boxes:

1 - Wavetec Signal Generator (Model #112)

1 - Blue Box (See following text)

1 - Spectroscopy Amplifier (ORTEC Model 450 or 451)

1 - ORTEC 420A Single Channel Analyzer (or Model 455)

1 - Count rate meter (ORTEC Model 441)

1 - Operational Amplifier (PAR Model 215)

1 - Multiplier (PAR Model 230)

2 - Gate and Delay Generators (ORTEC Model 416A)

1 - Oscilloscope

The magnet control box (Blue Box) is driven by the Wavetec signal generator. The magnet temperature sensor input (labeled pickup) must be shorted to ground in order to get any output from the Blue Box. A sweep wave is chosen (generally a triangle mode) and input to the magnet control box. With the Wavetec set at a frequency near 100 Hx either output of the magnet control is sampled and adjusted so that it remains positive with respect to ground.

Once this adjustment is made, the 10 V output can be connected to the Perkin current supply. Locate the adapter box in the back of the cabinet holding the quadrupole current controls. This is in the cyclotron control room and has a helipot mounted on it. Make sure that the box is properly connected to the wires leading to the Perkin control. The wire is 3 conductor and color coded with the terminals on the adapter.

If the wire is not on the adapter, it probably is connected to the terminals marked 3TB-10, 11, and 12 in the quadrupole helipot cabinet (See Figure 34).

Connection of the adapter box with the magnet conversion box is

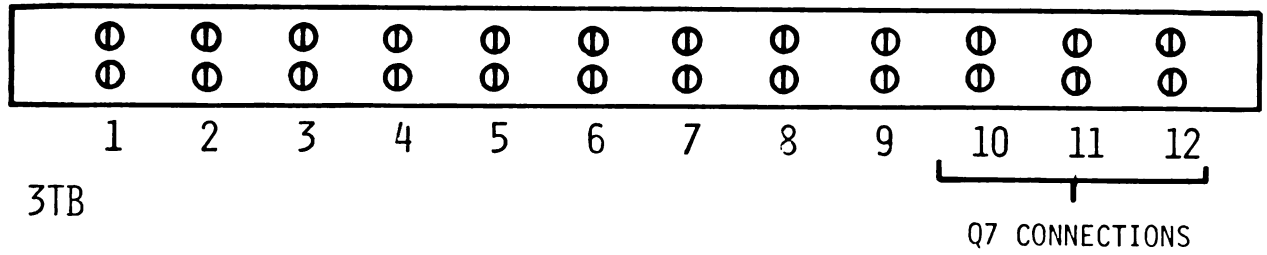

Figure 34. Magnet Control Connections

facilitated by using one of the control data connections in the data room located below the connectors from vault 2.

Now see that the temperature sensor is mounted properly on the water output clamp. This clamp is easily identified by the large amount of silicone grease which is usually smeared over it or by its black color. Plug a cable into the BNC Connector attached to the sensor. IMPORTANT: BE SURE THAT THE CABLE IS CONNECTED TO THE SENSOR FIRST AND THAT THE CABLE IS NOT IN ELECTRICAL CONTACT WITH THE PERKIN CURRENT LEAD. Grounding the current lead causes the Perkin current supply to shut off (it blows a fuse), usually causing the current cyclotron user to become very irritated. (Of course this phenomenon can be used to indicate a mistake has been made). Once it is determined that there is no danger of shorting the Perkin current supply, the cable can be connected to the pickup input of the magnet control box. Adjust the Wavetec to obtain a cycle period of about 100 seconds. Turn Q7 on and adjust the knob on the adapter box until the current read out corresponds to the maximum current needed to see the energy region of interest (solid line on graph). Because the spectrometer uses the leads for Q7, this quadrupole cannot be used for focusing the beam.

Leave the magnet running and take the oscilloscope into the experiment area of vault 2. Observe the output of the spectroscopy amplifier and adjust the gain. Then, triggering the oscilloscope from the single channel analyzer, turn the lower level discriminator knob until the pulse corresponding to a known gamma-ray energy just disappears. Record this voltage for later reference. Then turn the knob down to zero. When the SSCA is used for momentum selection, the recorded voltage is used to calibrate the sweep.

If the program "TOOTSIE" is to be used, refer to the Using "TOOTSIE" section. If the single channel analyzer is to be used, sample the output of the operational amplifier with the oscilloscope. The signal amplitude (negative) should correspond to the maximum energy pulse height as taken from the graph (dotted line) in Figure 21. (Note: This will have to be adjusted per any gain change). For example, suppose the maximum magnet current is 20 mV as determined by the Q7 readout and the 975 line from ^{207}Bi is 5.00 volts high at the bipolar output of the spectroscopy amplifier. From the graph the maximum energy seen by the magnet is 1,950 keV which corresponds to a pulse height of 10.00 volts. The SSCA output is then connected to the enable output of the ADC and a source spectrum taken for calibration.

3. Using "TOOTSIE"

"TOOTSIE" is a 2-parameter pulse height analysis program that allows the experimenter to store data with regards to both signal parameters. When first called by teletype command, the program is in the 2-D mode and counts are stored in a 64 x 256 matrix that is displayed on the storage scope. A point is displayed when the number of counts in that matrix element is between limits set by the programmer using the switch panel below the storage scope.

The signal from the amplifier is adjusted so that it stays between 0 and -6 volts on the oscilloscope. It is then fed directly into the unipolar input of the right analog-to-digital converter. No terminator is used.

The output from the gate and delay generators, having been adjusted in the vault 2 are input to the enable BNC plugs on the two analog-to-

digital converters. Set up the oscilloscope to trigger on one of the gate and delay pulses and observe the gated clock outputs under the code "POLYPHEMUS". Adjust the width of the gate enabling the right ADC until the start of the clock pulses from both ADC's are within 1 microsecond of each other. Exit "POLYPHEMUS" and call up "TOOTSIE". Take data until a definite pattern appears. This pattern should be an ever widening window. Using the switches divide the matrix into three regions, one of them enclosing this window (see Figure 21). Once the regions appear satisfactory, switch "TOOTSIE" over to the run mode. The data will be collected in one region and unwanted background in the other.

LIST OF REFERENCES

LIST OF REFERENCES

Av 73 Avignone III, R.T.; Pinkerton, J.E.; and Trueblood, J.H., "Combination Magnetic Si(Li) Swept Current Electron Spectrometer For On-Line Internal Conversion Spectroscopy," Nuclear Instruments And Methods No. 107 (1973): 453-59.

Ba 71 Bayer, D.L., "The Data Acquisition Task TOOTSIE," Computer Program (1971) Michigan State University Cyclotron Laboratory - 34.

Bl 52 Blatt, J.M. and Weisskopf, V.F., Theoretical Nuclear Physics New York: John Wiley and Sons, 1952.

Bl 66 Blosser, H.G. and Galonsky, A.I., "The Michigan State University 55 MeV Cyclotron: Progress and Status, February 1966," IEEE Transactions On Nuclear Power, NS-8, No. 4 (1966): 466-68.

Br 64 Brady, F.F.; Peek, N.F.; and Warner, R.A., "Energy Levels From Electron Conversion in ^{207}Pb," Crocker National Laboratory - Department of Physics, University of California, Davis (1964) CNL-UCD 23.

Ch 72 Chemical Rubber Co., Handbook Of Chemistry And Physics, 52nd Edition, 1972.

Go 74 Gono, Y. and Sugihara, T.T., "Electric Monopole Admixtures In Interband Transitions of ^{154}Gd," Physical Review C Vol. 10, No. 6 (1974): 2460-66.

Ha 68 Hager, R.S. and Selzer, E.C., "Internal Conversion Tables: Part 1," Nuclear Data Vol. A4, No. 1 and 2.

Kh 73 Khoo T.L.; Bernthal, F.M.; Boyno, J.S.; and Warner, R.A., "Experimental Demonstration Of Backbending Behavior From A Band Crossing in ^{154}Gd," Physical Review Letters Vol. 31, No. 18 (1973): 1146-49.

Le 67 Lederer, C.M.; Hollander, J.M.; and Perlman, I., Table of Isotopes, 6th Edition, New York: John Wiley and Sons, 1967.

No 73 Nolen, J.; Raut, H.; and Tody, D., "Target Fabrication," Michigan State University Cyclotron Laboratory, 1972-73.

Ro 58 Rose, M.E., Internal Conversion Coefficients New York: Inter-Science Publishers, Inc., 1958.

Si 55 Siegbahn, K., Beta- and Gamma-Ray Spectroscopy New York: North-Holland Publishing Co., 1955.

Wy 71 Wyckoff, W.G., "In-Beam Conversion Electron Studies of $^{72, 74, 76, 78}$Se, $^{78, 80, 82, 84}$Kr, $^{114, 116, 118, 120, 122, 124, 126}$Te, and $^{130, 132, 134, 136, 138}$Ce Utilizing (alpha, xn) Reactions," Ph.D. Dissertation, (1971) University of California-Davis (Unpublished).